UNIVERSITY OF CALIFORNIA SAN DIEGO

SAN DIEGO STATE UNIVERSITY

Microbial Ecology of the CF Lung

A dissertation submitted in partial satisfaction of the requirements for the degree
Doctor of Philosophy

in

Biology

by

Gregory Alan Willkeen

Committee in charge:

University of California San Diego

Professor Douglas J. Conrad

Professor Justin R. Meyer

San Diego State University

Professor Forest L. Rohwer, Chair

Professor Cristal Zúñiga, Co-Chair

Professor Barbara Bailey

Professor Anca M. Segall

2024

The dissertation of Gregory Alan Willkeen is approved, and it is acceptable in quality and form for publication on microfilm and electronically.

_____

_____

_____

_____

_____
Chair

_____
Co-Chair

University of California San Diego
San Diego State University

2024

EPIGRAPH

If you ordered scientists to form a firing line… they would make a circle.

Gregory Alan Willkeen

TABLE OF CONTENTS

LIST OF FIGURES

ACKNOWLEDGEMENTS

Chapter 1, in part, is currently being prepared for submission for publication of the material. Dunham, Sage J. B.; Whiteson, Katrine L.; Rohwer, Forest; Hahn, Andrea; Widder, Stefanie; Quinn, Robert A.; Bean, Heather D.; Klapper, Isaac; Thornton, Christina; Caverly, Lindsay; LiPuma, John J.; Martin, Christian; Wagner, Brandie D.; Bailey, Barbara A.; Corley, Jodi M.. The dissertation author was the primary researcher and author of this material.

Chapter 2, in part, is currently being prepared for submission for publication of the material. Canto-Encalada, Gabriela; Julazadeh, Hana; Bailey, Barbara A.; Rohwer, Forest; Zúñiga, Cristal. The dissertation author was the primary researcher and author of this material.

Chapter 3, in part, is currently being prepared for submission for publication of the material. Julazadeh, Hana; Souza, Cole; Segall, Anca M.; Rohwer, Forest. The dissertation author was the primary researcher and author of this material.

VITA

2013 Bachelor of Arts, International Relations, Florida International University

2013-2018 U.S. Army Airborne Field Artillery Officer, 173rd Airborne Brigade

2018-2024 Graduate Student, San Diego State University, Cell & Molecular Biology

2024 Doctor of Philosophy, Biology, San Diego State University & University of California San Diego

PUBLICATIONS

Cobián Güemes AG, Le T, Rojas MI, Jacobson NE, Villela H, McNair K, et al. Compounding Achromobacter Phages for Therapeutic Applications. Viruses. 2023;15: 1665. doi:10.3390/v15081665

Robinson M, Gilbert SF, Waters JA, Lujano-Olazaba O, Lara J, Alexander LJ, et al. Characterization of SOX2, OCT4 and NANOG in Ovarian Cancer Tumor-Initiating Cells. Cancers. 2021;13: 262. doi:10.3390/cancers13020262

FIELDS OF STUDY

Major Field: Biology (Microbiology)

ABSTRACT OF THE DISSERTATION

Microbial Ecology of the Cystic Fibrosis Lung

by

Gregory Alan Willkeen
Doctor of Philosophy in Biology
University of California San Diego, 2024
San Diego State University, 2024

Professor Forest L. Rohwer, Chair
Professor Cristal Zúñiga, Co-chair

Cystic Fibrosis (CF) is an autosomal recessive disorder caused by mutations to the Cystic Fibrosis Transmembrane-conductance Regulator (CFTR) gene, that leads to the buildup of thickened mucus in the lungs that are chronically infected by bacteria (often antibiotic resistant) and fungi. These chronic infections periodically flare in acute events called pulmonary exacerbations which leads to scarring of the lung and permanent decline in pulmonary function. This work presents a model of CF

lung disease that incorporates the taxonomic diversity observed in the CF lung into ecological guilds based on their role in the CF sputum environment, resulting in the proposal of four functional groups called the Brewers (fermenting microbes), Drunkers (biofilm building consumers of fermentation products), Putrifiers (anaerobic biofilm dwelling bacteria) and Nihilists (lone wolf pathogens of the lung). Another model of the CF lung microbiome, found in this dissertation, predicts the succession of bacteria in CF sputum based on the concentration of succinate found in the sputum environment, which is known to be substantially higher than sputum from people without CF. The second model is based on the differential succinate flux values predicted by GEnome scale metabolic Models (GEMs) for the 29 most prevalent bacterial species in the CF lung, and observations of in vitro growth data of a mock community of four CF isolated strains of bacteria. The results of which support the existence of two distinct consortia of bacteria in the CF lung, consortium 1 made up of typical CF pathogens which can metabolize succinate and consortium 2 which contains bacteria associated with the human oral cavity that do not metabolize succinate and are likely inhibited by succinate at high concentrations. Lastly, with the aim to address the issue of treating antibiotic resistant bacterial infections in patients with CF or otherwise, this dissertation presents two engineered tailocins MobyWanKenobi and John Henry, that bind to and kill CF isolated strains of *Stenotrophomonas maltophilia* and both *Staphylococcus aureus* and *Serratia odorifera* respectively.

INTRODUCTION

Cystic fibrosis is an autosomal recessive disorder caused by mutations to the cystic fibrosis transmembrane conductance regulator gene that result in no protein production or the generation of a dysfunctional protein. One of the results of the lack of this functioning protein is the buildup of thick mucus in the lower airways (Riordan et al., 1989). Diverse microbes inhabit the lungs of People with Cystic Fibrosis (pwCF), forming complex communities that influence the health of each CF patient. Although these microbes have been identified and cataloged over decades of research (Thornton et al., 2023), CF researchers are still learning what each microbial species does in the lung and how their actions affect lung function and patient health. It is known that certain microbial species in CF lungs perform similar functions, and can affect each other's functioning, though the precise mechanisms underlying such interactions are unclear.

In addition, Cystic Fibrosis investigators need to adapt to the widely adopted and successful use of Cystic Fibrosis Transmembrane conductance Regulator (CFTR) modulator (trikafta) therapy (Fajac & Sermet-Gaudelus, 2021). This change to the CF patient population indicates that a shift to personalized medicine for the estimated 10% of non-responder CF patients is now a real possibility and will likely require the participation of the research community. This will require using multi-omics data to inform physicians of the disposition of the microbes in the patient's airways (Cobián Güemes et al., 2019a; Silveira et al., 2021) and second, the actual

production of novel personalized treatments (Bradley et al., 2023; Passi et al., 2022). To address the first example of researcher-physician collaboration towards personalized medicine, chapter one of this dissertation proposes a microbial guild-based model of CF airway disease. Chapter 1 posits that the field of CF lung researchers would benefit from a transition from a taxonomy-based model of CF microbial ecology to a guild-based model that incorporates many taxa into groups based on resource utilization, production, metabolite exchange and niche construction. Four distinct guilds are described according to their metabolic function in the CF lung as well as which niche each guild exploits as well as the niche that each guild constructs for the other microbes of the CF lung.

Chapter 2 of this work focuses on the fact that the lungs of people with cystic fibrosis have high concentrations of succinate, which has been shown to support growth of the CF pathogen *Pseudomonas aeruginosa* (Riquelme et al., 2019) and how this high concentration of succinate affects the microbial ecology of the CF lung. Chapter 2 tested whether succinate was able to support growth of additional CF microbes and identified two bacterial consortia differentially affected by the presence of succinate. Results from analyzing metagenomic sequences from over 20 patients, genome-scale metabolic modeling, and *in vitro* growth experiments suggest that succinate concentrations may dictate microbial dynamics in the CF lung, where a succinate-utilizing community depletes succinate, enabling growth of a succinate-intolerant community. This work updates the Climax-Attack Model of CF lung

microbial ecology (D. Conrad et al., 2013a) that posits two distinct communities of bacteria inhabit the CF lungs and differentially affect patient health.

In chapter three this work proposes engineered tailocins that kill antibiotic resistant pathogens of the CF airways as the second way that the CF research community can provide potentially better options to physicians treating patients that are not eligible for trikafta. Tailocins are bacteriophage tail remnants that have potential as targeted bactericidal therapeutics (D. W. Jr. Martin et al., 2010; Ritchie et al., 2011; Scholl et al., 2009; Scholl, 2017; Williams et al., 2008). Two tailocins, Moby-WanKenobi and John Henry, were engineered to target *Stenotrophomonas maltophilia* and gram-positive and gram-negative bacteria, respectively. These tailocins were engineered by fusing the tail spike from myophage Moby or the human Carbohydrate Recognition Domain of Mannose-Binding Lectin, respectively, with the *Pseudomonas aeruginosa* R2 pyocin tail fiber. This fusion approach, developed to engineer the *E. coli* O157:H7-specific tailocin Avidocin (Scholl et al., 2009), shows great promise for targeted tailocin design.

CHAPTER 1 A guild model of CF Airway Microbial Ecology

It's time to pivot our approach to CF airway microbial ecology.

Cystic fibrosis transmembrane conductance regulator (CFTR) modulator therapies (Trikafta, elexacaftor-tezacaftor-ivacaftor) have dramatically changed the medical outcome of CF lung disease, with an estimated 90% of people with CF (pwCF) eligible for Highly Effective Modulator Therapy (HEMT) therapy (Cystic Fibrosis Foundation, 2021; Fajac & Sermet-Gaudelus, 2021). Even with this dramatic shift, pervasive microbial infection and inflammation of the airways continues to be the leading cause of death in pwCF. Over the last decade, microbial ecologists have generated large multi-omic datasets of CF airway microbes, attempting to understand the relationship between disease state and the microbiome, and to provide clinically relevant advice on how to avoid pulmonary exacerbations and improve quality of life (Boucher, 2004; Castner et al., 2021; K. Chen & Pachter, 2005; Cobián Güemes et al., 2019b; D. Conrad et al., 2013b; D. J. Conrad et al., 2017; D. J. Conrad & Bailey, 2015; Cuthbertson et al., 2020; Flynn et al., 2016; Garg et al., 2017; Lim, Schmieder, Haynes, Furlan, et al., 2013; Lim, Schmieder, Haynes, Willner, et al., 2013; Lim et al., 2014; Lu et al., 2020; Melnik et al., 2019; Quinn et al., 2014, 2015a; Quinn, Lim, et al., 2016; Quinn, Phelan, et al., 2016; Quinn, Whiteson, et al., 2016; Quinn et al., 2018, 2019; Sahu & Lynn, 1978; Scoffield & Silo-Suh, 2016; Sriramulu et al., 2005; Stressmann et al., 2011; Stuart Elborn et al., 2015; Tavernier et al., 2017; Theilmann

et al., 2016; Whiteson, Bailey, et al., 2014; Whiteson, Meinardi, et al., 2014a; Willner et al., 2009; Willner, Haynes, Furlan, Hanson, et al., 2012; Willner, Haynes, Furlan, Schmieder, et al., 2012; Worlitzsch et al., 2002; Zarei et al., 2012, 2014). This work proposes a conceptual shift in how researchers assess the CF airway microbiome that still holds relevance in the era of HEMT (C. Martin et al., 2023), moving away from prior, largely taxonomical approaches, towards a guild-based model. Ecological guilds are groups of taxonomically distinct entities that utilize the same class of resources from their environment (Simberloff & Dayan, 1991). Guilds of microbes are defined by the functional character of their protein coding sequences (Rivas-Santisteban et al., 2023). A guild model for CF airway ecology relies on the ecological function of each microbe and considers the role that the organism plays in the context of the wider community and environment. We propose four guilds to which the microbes are broadly classified: 1) Brewers, which are largely facultative anaerobic or microaerobic organisms that metabolize mucins and produce fermentation products, 2) Drunkers, are opportunistic pathogens, which exploit the metabolic niche built by the Brewers, consuming the fermentation products and secreting exopolysaccharides to build biofilms, 3) Putrifiers are opportunistic pathogens, which are anaerobic bacteria that produce toxic compounds that lead to local inflammation and tissue necrosis, and 4) Nihilists are specialist pathogens, which are characterized by intracellular or lytic lifecycles and the production of cytotoxic proteins. By considering function and the broader community context, we can build a more informed understanding of airway ecology and apply that knowledge to improve the care of pwCF (Cobián Güemes et al., 2019b).

1.1 What needs to change to make this possible?

CF airway microbial ecology needs to shift away from attempts to construct a model of CF lung disease based on bacterial taxonomy and instead transition to a guild-based model (Moyne et al., 2023). This requires sorting the diverse microbial communities of CF airway microbes into distinct guilds based on metabolism and function rather than genetic similarity. (Figure 1.1) Current evidence indicates that CF airway communities can be categorized into four broad functional groups based on utilization of two key resources: oxygen and mucin. Under normal circumstances, mucin and oxygen are both theoretically infinite resources from the microbe's perspective since mucin is continually generated by the human host and oxygen-rich air is drawn into the lungs by breathing. However, as mucus plugs form in the CF lung, both of these resources become limited (Panchabhai et al., 2016). Microbes break down the available mucin and deplete oxygen (Quinn et al., 2015a). The chain of resource utilization starts with the first functional group in our model, the 'Brewers'. Brewers are defined by their ability to metabolize mucin and make nutrients available for other microbes, either by liberating mucin glycochains or producing short chain fatty acids. Examples include eukaryotic opportunistic pathogens such as *Candida spp.*, which produce serine proteases that can cleave mucin chains, freeing the sialic acid and fucose for consumption by itself and other microbes (Colina et al., 1996). Prokaryotic brewers can be facultatively anaerobic or anaerobic bacteria such as *Streptococcus spp.* or *Staphylococcus spp.* that produce nutrients such as short

chain fatty acids or lactate as a byproduct of their metabolism (Crouch et al., 2020; Marchandin et al., 2010; Yamada & Carlsson, 1975).

A key feature of the Brewers is that they make energy available in the form of organic and short chain fatty acids for the second guild of microorganisms, called 'Drunkers', which are biofilm-producing bacteria such as *Pseudomonas spp.*, *Achromobacter spp.* or *Stenotrophomonas spp.* Drunkers exploit the metabolic niche built by the Brewers and in turn build another niche (a biofilm) by secreting alginate or other exopolysaccharides into the mucus plug. Those exopolysaccharides facilitate the aggregation of microbes into a complex and densely packed matrix (A. I. Chen et al., 2014; Gebreyohannes et al., 2019; May et al., 1991; Scoffield & Silo-Suh, 2016; Sønderholm et al., 2018; Sriramulu et al., 2005; Tavernier et al., 2017). Drunkers are also susceptible to being induced into biofilm formation by other fermentation products from the Brewers such as 2,3-butanediol or ethanol (A. I. Chen et al., 2014; Nguyen et al., 2016; Silveira et al., 2021; Whiteson, Meinardi, et al., 2014b). Which can lead to increased colonization of the airways as well as persistence through antibiotic treatments (Gebreyohannes et al., 2019; Kandel et al., 2020).

Once the accumulated metabolism of the Brewers and Drunkers depletes enough oxygen and lowers the pH, the next functional group, the 'Putrifiers', begins to proliferate. Putrifiers are bacteria characterized by anaerobic metabolism such as *Prevotella spp.* and *Veillonella spp.*. Anaerobic metabolism by Putrifiers results in the production of toxic compounds such as putrescine and spermidine, which can cause

local inflammation and necrosis (del Rio et al., 2019; Rogers et al., 2015). Putrescine has been observed between 100 - 600 μM in CF sputum around the time of pulmonary exacerbation, which is approximately an order of magnitude greater than what is reported in CF sputum during periods of clinical stability (approximately 25 μM) (Grasemann et al., 2012; Twomey et al., 2013). Putrifiers can also cause tissue damage via the secretion of collagenases (Damé-Teixeira et al., 2018). Lactate has also been reported at elevated levels in CF sputum during exacerbation, approximately 400 μM compared to 26 μM in stable CF sputum (Twomey et al., 2013). The interplay between Brewers, Drunkers, and Putrifiers described above results in the progressive lung damage and loss of respiratory function that characterizes CF.

The final guild is a group of stand-alone pathogens, the ‘Nihilists’. This group is a loose collection of viruses and bacteria that are independently cytotoxic, cytolytic or carry out intracellular life cycles. Nihilists include adenoviruses, which lyse human cells as a part of their life cycle (Jiang et al., 2011), or bacteria like *Streptococcus pyogenes*, which produce hemolysins that rupture red blood cells (Kinsella & Swift, 1918). This cohort of Nihilists is thought to be capable of instigating inflammation and lung damage in CF patients without the need to engage with the rest of the guilds present in the CF lung. Many of these pathogens can also cause pulmonary infections in otherwise healthy people, such as SARS-CoV-2 which can cause acute respiratory infections (Bar-On et al., 2020; Ciotti et al., 2019) or *Bordetella pertussis* which causes Whooping Cough (Norton & Bailey, 1931).

Rather than including every possible scenario of these microbial guilds' actions and interactions, this work proposes a guild model as a shift in how the CF research community thinks about the establishment and succession of CF lung infections, pulmonary exacerbation, and progressive lung disease. Hopefully this model will provide a framework for hypothesis generation and experimental design for the CF research community as we move forward. Using four guilds rather than distinct taxonomic units can help scientists reduce the noise and dimensionality of their datasets, thereby enabling them to make sense of the ecological dynamics at play.

Figure 1.1: Guild model of CF lung ecology featured in a painting of the progression of CF lung disease. This figure seeks to use functional categories of CF pathogens (which are based on metabolism) to explain short and long term progression of CF lung disease. Panel 1,The Normal Human Airway: Is a healthy lung with mucins flowing freely over lung epithelial cells. Beating cilia move the mucus, which carries debris and microbes with it, out of the lungs. The high turnover rate of mucins (comprising electron donors) and the flow of mucus makes this environment difficult to colonize. Panel 2, Equal Opportunity Nihilists: Is an otherwise healthy lung being invaded by a member of the non-CF specific guild, the 'Nihilists'. Nihilists are lone wolf pathogens that are characterized by intracellular lifecycles, lytic lifecycles, or the production of cytotoxic proteins. We are depicting a respiratory virus invading a healthy lung and killing the epithelial cells, causing a pulmonary exacerbation. Panel 3, The Young CF Lung: Is the lung of a young pwCF, where the mucus is thick and recalcitrant due to the imbalance of divalent cations. This leads to a low mucin turnover rate as well as little to no mucus flow. This lung is ripe for colonization by the first CF-specific guild of pathogens, the 'Brewers'. Brewers are facultatively anaerobic/microaerophilic microbes that can metabolize the readily abundant mucins and produce the fermentation products, such as propionate or acetate, that feed the second guild of CF-specific microbes, the 'Drunkers'. The most common Brewers found in CF lungs are *Staphylococcus spp.*, *Streptococcus spp*. and *Candida spp*. (yeast). *Candida* secretes mucolytic serine proteases, which degrade mucins, thereby enabling their consumption by *Candida* and other microbes. Yeast produce fermentation products, like ethanol, which induce biofilm formation in the 'Drunkers'. Drunkers are biofilm-building bacteria, such as *Pseudomonas spp*., that secrete alginate and shuttle electrons from fermentation products to O_2 (from air or blood) when available, or to alternate electron acceptors like nitrate or sulfate. Panel 4, The mucus plug: This image is a lung containing all three of the CF-specific guilds: Brewers, Drunkers and Putrifiers. Brewers are producing enough fermentation products to feed a large cohort of Drunkers. The Drunkers have secreted enough alginate to build a biofilm that is densely populated by bacteria that are lowering the oxygen concentrations until an anaerobic niche is built. This anaerobic niche is exploited by the third guild, the 'Putrifiers', which are anaerobic bacteria that produce toxic polyamines such as putrescine and spermidine as a byproduct of their metabolisms. These polyamines can cause inflammation and further neutrophil infiltration. As the neutrophils lyse to produce neutrophil extracellular traps (NETs), they cause a positive feedback loop of inflammation and the accumulation of human genomic DNA in the mucus. At high concentrations this DNA feeds the microbes and thickens the biofilm, thereby increasing recalcitrance.


Ben Darby

1.2 Incorporating existing datasets into the new conceptual framework.

To build out this conceptual model, a workflow is proposed in Figure 1.2 that outlines the analysis of sputum metagenomes. The workflow progresses from whole genome shotgun sequencing reads to the binning of microbes into guilds according to identified genes. The microbial genome uses broad brushstrokes to paint an image of the metabolic/energetic landscape of the cell, which is used to classify the organism into the categories of Brewer, Drunker or Putrifier. When metatranscriptomes or metabolomes are available for the same sputum sample they can improve guild classification by confirming the expression of key genes or the production of metabolic byproducts. Mobile genetic elements such as prophages and plasmids carry virulence genes (e.g., exotoxins, immune evasion, and antibiotic resistance) that allow a member of any of the primary three guilds to become Nihilists. For example, *E. coli* K12 (a laboratory strain that is generally regarded as safe for the production of recombinant enzymes to make cheese) could be converted to a high titer Shiga toxin producing strain by the prophages of an isolate of the notorious O157:H7 serogroup (O'Brien et al., 1984).

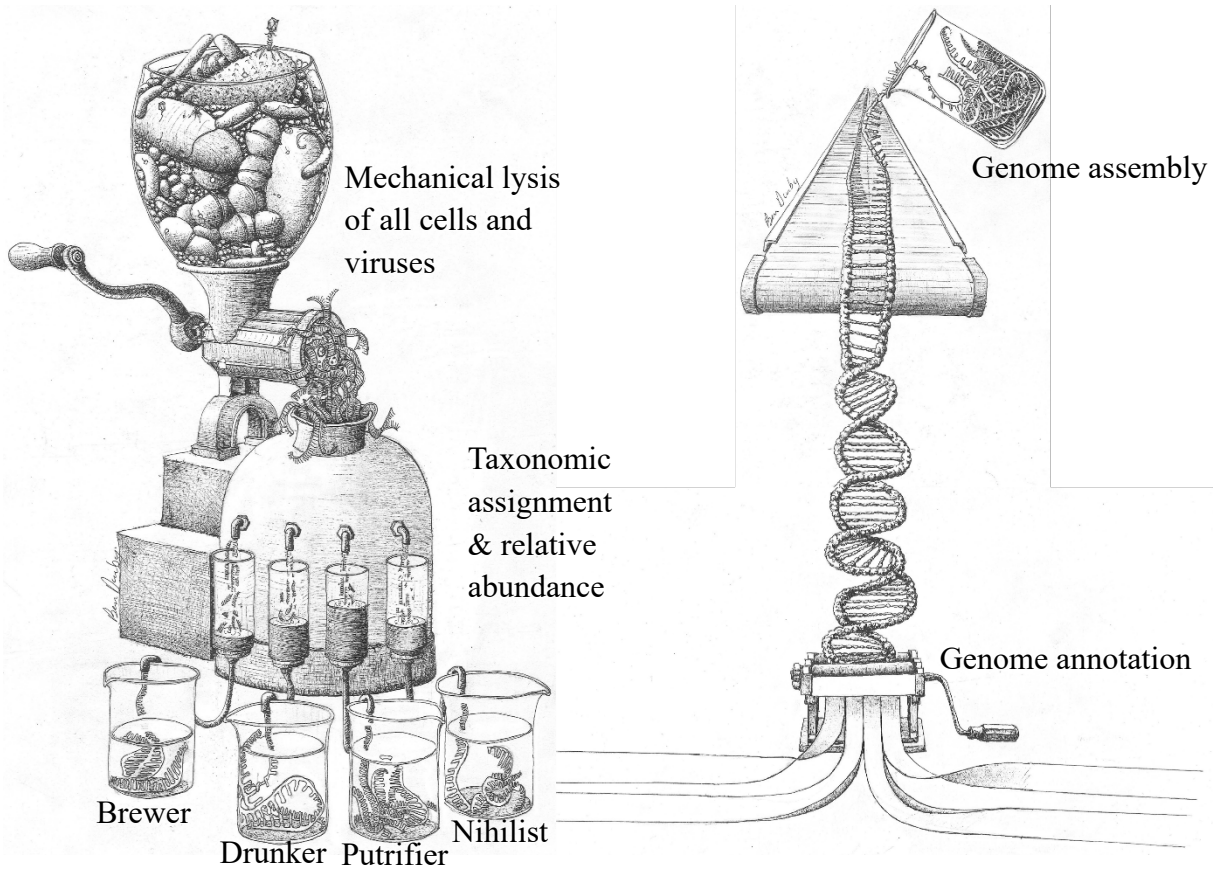

Figure 1.2: Decision tree for binning microbes into the four functional categories proposed by a guild model of CF lung ecology. The illustrated flowchart begins at the top left, where the sausage grinder represents the process of lysing all the bacteria, fungi and viruses found in the CF sputum in order to extract and sequence the DNA. Whole-genome shotgun (WGS) reads are processed and assigned to taxonomic units based on their identities to database sequences of known taxa. By counting those reads, after normalizing for genome size, one can determine the relative abundance of each species, this is depicted by the short pieces of DNA accumulating in the containers with the different volumes of liquid representing different relative abundances. Microbes of interest can be selected based on their relative abundances; their corresponding WGS reads should be binned before genome assembly, represented by the beakers filled with DNA. Binned reads then need to be assembled into contigs using their nearest relative as a scaffold, this is represented by the assembly-line conveyor belt with the binned reads being poured out of the beaker onto the assembly line. Once assembled the genome is then annotated. Each microbe can then be assigned to a guild according to the predicted functions of genes present in its genome.

1.3 Novel experimental models.

Researchers have struggled to find an effective animal model of CF, in large part because the models that best recapitulate the hallmarks of CF lung disease, such as ferrets and pigs are too expensive for large, statistically meaningful studies (McCarron et al., 2021). These constraints have led to the development of *in vitro* models using artificial CF sputum media, such as the WinCF model (Quinn et al., 2015b). The WinCF model and other *in vitro* models have shortcomings such as not being chemostats, not incorporating host immune cells, and employing an imperfect substitute for CF sputum as the medium (Quinn et al., 2015b). It is also worth noting that increasingly sophisticated genome-scale metabolic models raise the possibility of *in silico* modeling of the CF lung together with its resident microbial community (Orth et al., 2010; Passi et al., 2022). Moving forward, CF researchers need to improve both our *in vitro, in vivo*, and *in silico* models to serve the personalized needs of pwCF (O'Toole et al., 2021). Ideally, these models would allow researchers to effectively and affordably test hypothetical treatments tailored towards the needs of each person with CF to impact their airway microbial community and improve their quality of life. In order to have confidence in the relevance of a model of CF, quantitative validation of the model in comparison to sputum from a pwCF would enable us to understand which parts of their model successfully recapitulate infection. This could be accomplished by comparing metagenomic, metatranscriptomic and metabolomic similarity of their model to sputum from pwCF (Cornforth et al., 2020).

1.4 Conclusion.

There remains a need for practical, safe, and personalized recommendations to treat airway infection in pwCF. Whereas antibiotics continue to be the mainstay of therapy, other approaches such as phage and mRNA therapy are being explored (Bradley et al., 2023; Da Silva Sanchez et al., 2020; *mRNA Therapy for Cystic Fibrosis | Cystic Fibrosis Foundation*, n.d.; Rowe et al., 2023; Winzig et al., 2022). As CF researchers and care providers, we need to design models to understand how those therapies will affect CF microbial community dynamics and look for ways to exploit the principles of microbial ecology to reduce disease burden in individuals with chronic antibiotic resistant infections. This requires us to design experiments that assess the presence and activity of the four major guilds; the Brewers, Drunkers, Putrifiers, and Nihilists. This guild model is proposed to help researchers and physicians simplify interpretation of CF infection composition through the reduction of taxonomic complexity. A model community could theoretically consist of only three to four microbes (representing each guild), yet still allow researchers to test the effect of those treatments on CF microbial community dynamics.

Chapter 1, in part, is currently being prepared for submission for publication of the material. Dunham, Sage J. B.; Whiteson, Katrine L.; Rohwer, Forest; Hahn, Andrea; Widder, Stefanie; Quinn, Robert A.; Bean, Heather D.; Klapper, Isaac; Thornton, Christina; Caverly, Lindsay; LiPuma, John J.; Martin, Christian; Wagner,

Brandie D.; Bailey, Barbara A.; Corley, Jodi M.. The dissertation author was the primary researcher and author of this material.

CHAPTER 2 Succinate metabolism partitions microbial communities into metabolically distinct consortia in Cystic Fibrosis lungs

Cystic Fibrosis (CF) is an autosomal recessive disorder caused by mutations to the Cystic Fibrosis Transmembrane conductance Regulator (CFTR). These mutations disrupt normal anion transport across epithelia and in the lung result in thick airway mucus and decreased mucociliary clearance. This allows the growth of a chronic polymicrobial airway biofilm infection. This infection can flare (a CF pulmonary exacerbation) which causes more inflammation and accelerated airway scarring and loss of lung function. In addition to altered mucus, mutated CFTR cannot complex with the PTEN tumor suppressor protein, resulting in the mitochondria producing excess succinate that favors growth of *Pseudomonas aeruginosa*, and reactive oxygen species that induce inflammation in the lung airways (Riquelme et al., 2019). Although Gram-positive bacteria typically cannot metabolize succinate (Richardson et al., 2015), many Gram-negative CF pathogens, in addition to *P. aeruginosa*, are likely to use succinate as a carbon source in the lung airways.

The Climax and Attack model (CAM) of CF lung disease applies principles of succession from the field of ecology to the microbial dynamics of the CF sputum. CAM predicts that a resident community of host-adapted microbes (Climax community) is displaced by a community of non-resident microbes that are more pathogenic and cause acute inflammation and pulmonary exacerbation (Attack community) (D. Conrad et al., 2013a). However, the metabolic capabilities of the

Climax and Attack communities, and how they may take advantage of excess succinate, are not known.

To test the hypothesis that succinate contributes to niche differences that select for Climax versus Attack communities, metagenomic analysis, metabolic modeling, and in vitro growth experiments were performed. The results indicate the existence of two consortia within the CF lung: consortium 1, which could potentially function as a Climax community, metabolizes succinate to enable its community dominance; once succinate is locally depleted, consortium 2, the Attack community, increases in abundance, potentially leading to exacerbation.

2.1 Results

Predicted metabolism and abundance data reveal two microbial consortia in CF.

The Climax-Attack Model predicts that the Climax and Attack communities of bacteria in the CF lung differ in their ecological function, which could include differences in succinate metabolism. Thus, GEnome scaled Metabolic models (GEMs) were used to investigate potential metabolic differences between bacteria commonly associated with the CF lung. A GEM simulates an organism's metabolism based on niche constraints using the enzymes predicted to be encoded by the genome, follow-on metabolites and associated genes from all metabolic reactions.

The Flux Balance Analysis (FBA) uses the GEM and associated constraints to generate growth simulations of an organism that result in a table of predicted flux values for each enzymatic reaction in the model (Orth et al., 2010). An automatically-generated metabolic model was built for each of 29 bacterial species found to be most common in samples of CF sputum using Kbase (Arkin et al., 2018). The 29 most prevalent species were determined by analyzing a set of 73 randomly selected CF sputum metagenomes from the Sequence Read Archive (SRA) for bacterial species with a z-score above 2 or prevalence above 25% within the 13 most prevalent bacterial genera described in (Thornton et al., 2023). Constraints used to perform the simulations are provided in Supplementary Table 2.1 Flux values for succinate and import values for oxygen were generated for each of the 29 species (Figure 2.1). A hierarchically clustered heatmap based on these predicted values showed two distinct clusters of taxa, or consortia. Consortium 1 comprised species that are considered typical CF pathogens, such as *Pseudomonas aeruginosa*, *Staphylococcus aureus*, *Achromobacter spp.* and *Stenotrophomonas maltophilia*. Consortium 2 featured oral cavity bacteria, including *Rothia mucilaginosa*, *Veillonella spp.*, and *Streptococcus spp.* (Figure 2.1).

To validate the relevance of those two consortia, 24 CF sputum metagenomes were randomly selected from the SRA for analysis (≈ 1% of available sputum metagenomes at the time of analysis) by randomizing a list of all available CF sputum metagenomes SRA accession numbers. A full description can be found in the methods section of this chapter under the “Metagenomics” subsection. Relative

abundances of the bacteria in Figure 2.2 were used to generate a hierarchically clustered heatmap of Spearman's correlation coefficients (Figure 2.1). This heatmap shows two distinct clusters or consortia that align with the 2 consortia identified in Figure 2.1. Furthermore, abundances of members within each consortium were inversely correlated with one another more strongly than they correlated with the other members of their own consortium. This is what one would expect since each randomly selected metagenome was likely from a different individual with a different dominant pathogen, e.g., *Pseudomonas* versus *Stenotrophomonas*. Consortium 1 and 2 were also recovered with smaller subsets of 5, 10 and 15 randomly selected sputum metagenomes from the 24 used in Figure 2.2. Thus, indicating a lack of sensitivity to the number of metagenomes selected for the analysis and the robustness of the inverse correlation between consortium 1 and consortium 2 in a given CF sputum metagenome. (Supplementary Figures 2.1, 2.2 & 2.3)

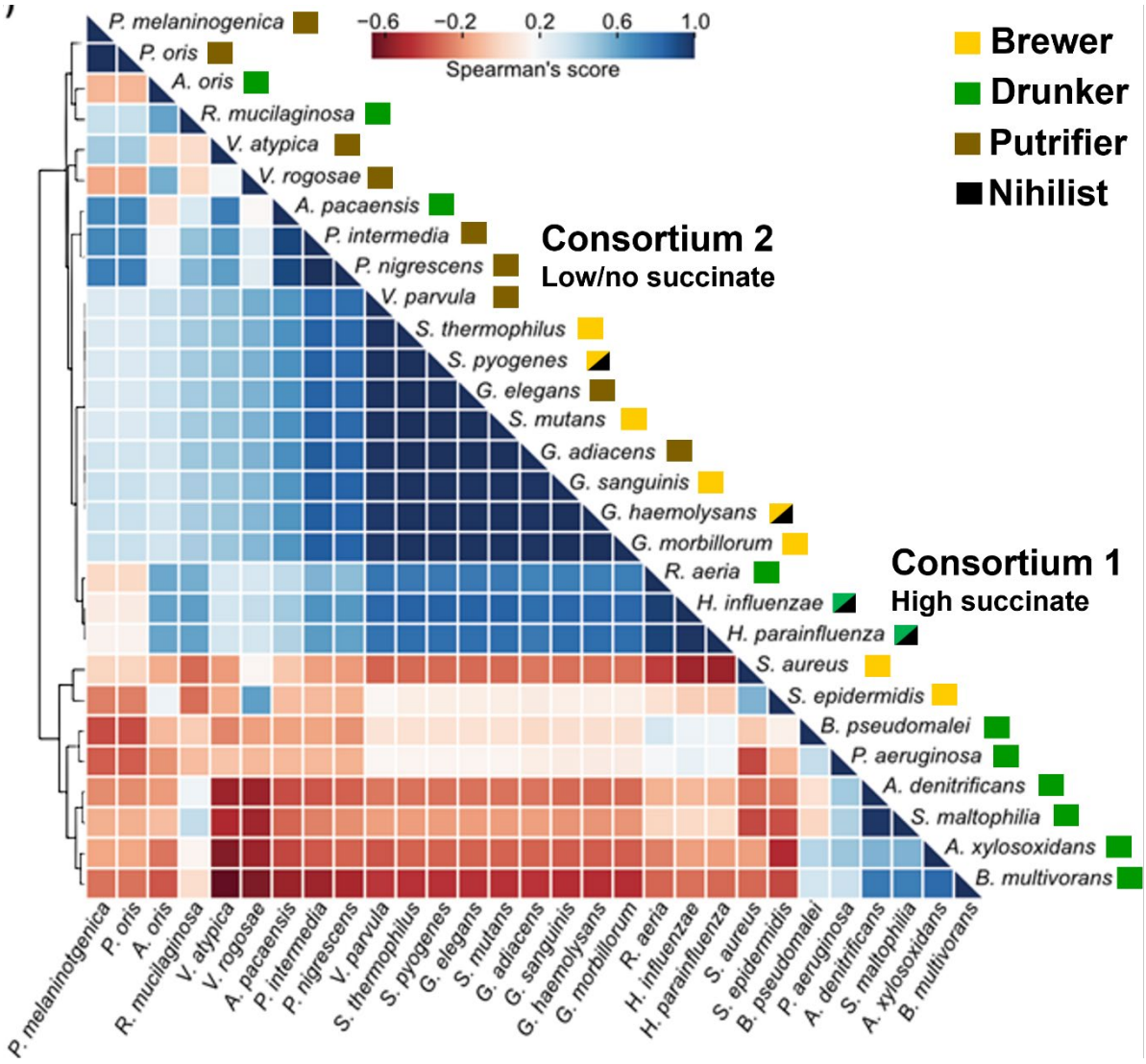

Figure 2.1: Bacterial genera cluster into two groups in a CF patient lung microbiome.A, Hierarchically clustered heatmap of Spearman's correlation coefficients, calculated using the z-scores of predicted succinate flux values and oxygen import values from GEMs generated in KBase for each of the 29 most prevalent bacterial species in the CF lung. Genus abbreviations are as follows: *P. aeruginosa* refers to *Pseudomonas,* while all other *P.* refer to *Prevotella. R.* refers to *Rothia, V.* refers *to Veillonella, A. pacaensis* refers to *Actinomyces,* and all other *A.* refer to *Achromobacter, S. thermophilus, pyogenes & mutans* refers to *Streptococcus*, while all other *S.* refer to *Staphylococcus*; *G. adiacens & elegans* refer to *Granulicatella*, all other *G.* refer to *Gemella, H.* refers to *Haemophilus, B.* refers to *Burkholderia.*

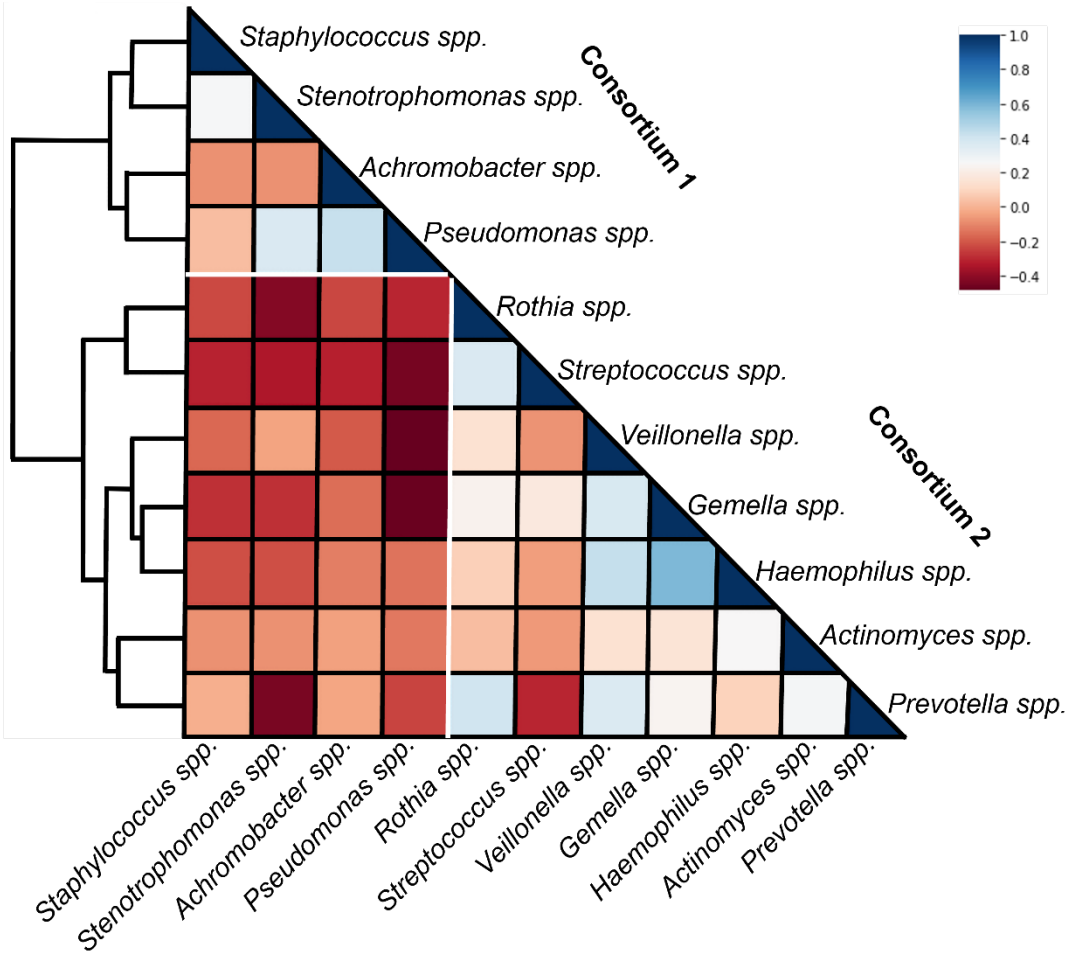

Figure 2.2: Hierarchically clustered heatmap of Spearman's correlation coefficients, calculated using the relative abundances of the 13 most prevalent genera of bacteria of the CF lung, as shown in (Thornton et al., 2023), from 24 randomly selected CF sputum metagenomes from the SRA.

Succinate potentially shapes consortium activity.

To validate the GEMs' predictions of succinate and lactate being differentially fluxed by members of the two consortia, *Achromobacter xylosoxidans, Streptococcus sanguinis,* and *Staphylococcus aureus* were isolated from one sample sputum

sample from a single CF patient and cultured in the presence or absence of succinate or lactate. An additional strain of *R. mucilaginosa*, previously isolated from a different CF patient, was also included to form a model CF microbial community for further *in vitro* analysis.

Pure cultures of consortium 1 members *A. xylosoxidans* and *S. aureus*, and consortium 2 members *R. mucilaginosa* and *S. sanguinis* were grown for 48 hours in BHI with increasing concentrations of succinate (0 mM to 500 mM; Figure 2.3 A&B). Consortium 1 members grew with or without supplemental succinate. *A. xylosoxidans* grew at a rate of ≈ 0.2 per hour in BHI without succinate and ≈0.12 in BHI with 125 or 250 mM succinate. At 500 mM, however, the growth rate declined to 0.02 with a maximum OD_{600} of 0.09. *S. aureus* grew at a rate between 0.27 to 0.55 as the concentration of succinate increased from 0 to 500. In contrast, consortium 2 members grew at a rate of ≈0.2 per hour in BHI without succinate and at rate of 0.02 at 125 mM of succinate. These results indicate that 125 mM was sufficient to prevent growth of consortium 2 members.

Figure 2.3: Effects of succinate and lactate on growth. A, Per hour growth rates of *A. xylosoxidans, S. aureus, R. mucilaginosa* & *S. sanguinis* as pure cultures, in BHI media supplemented with increasing concentrations of succinate. Box plots display growth rates from five iterations of the growth experiment, each with five technical replicate wells per experiment. B, Maximum optical density at 600 nm wavelength of *A. xylosoxidans, S. aureus, R. mucilaginosa* & *S. sanguinis* as pure cultures, in BHI media supplemented with increasing concentrations of succinate. Box plots display maximum optical density values from five iterations of the growth experiment, each with five technical replicate wells per experiment. C, Growth curves of a co-culture of patient isolated *A. xylosoxidans* and *S. aureus* (Consortium 1) in BHI or BHI + 250 mM succinate or lactate and a co-culture of CF isolated strain of *R. mucilaginosa* and the patient isolated strain of *S. sanguinis* (Consortium 2) in BHI or BHI + 250 mM succinate or lactate. Growth curves represents a single iteration of a growth experiment with 8 pseudoreplicate wells per condition (same colony used to innoculate each of the 8 replicate wells on one 96 well plate. Error bars for the growth curves are standard deviations of the values from the 8 replicate wells at the same timepoint (in most cases the deviation is too low to see the error bars).

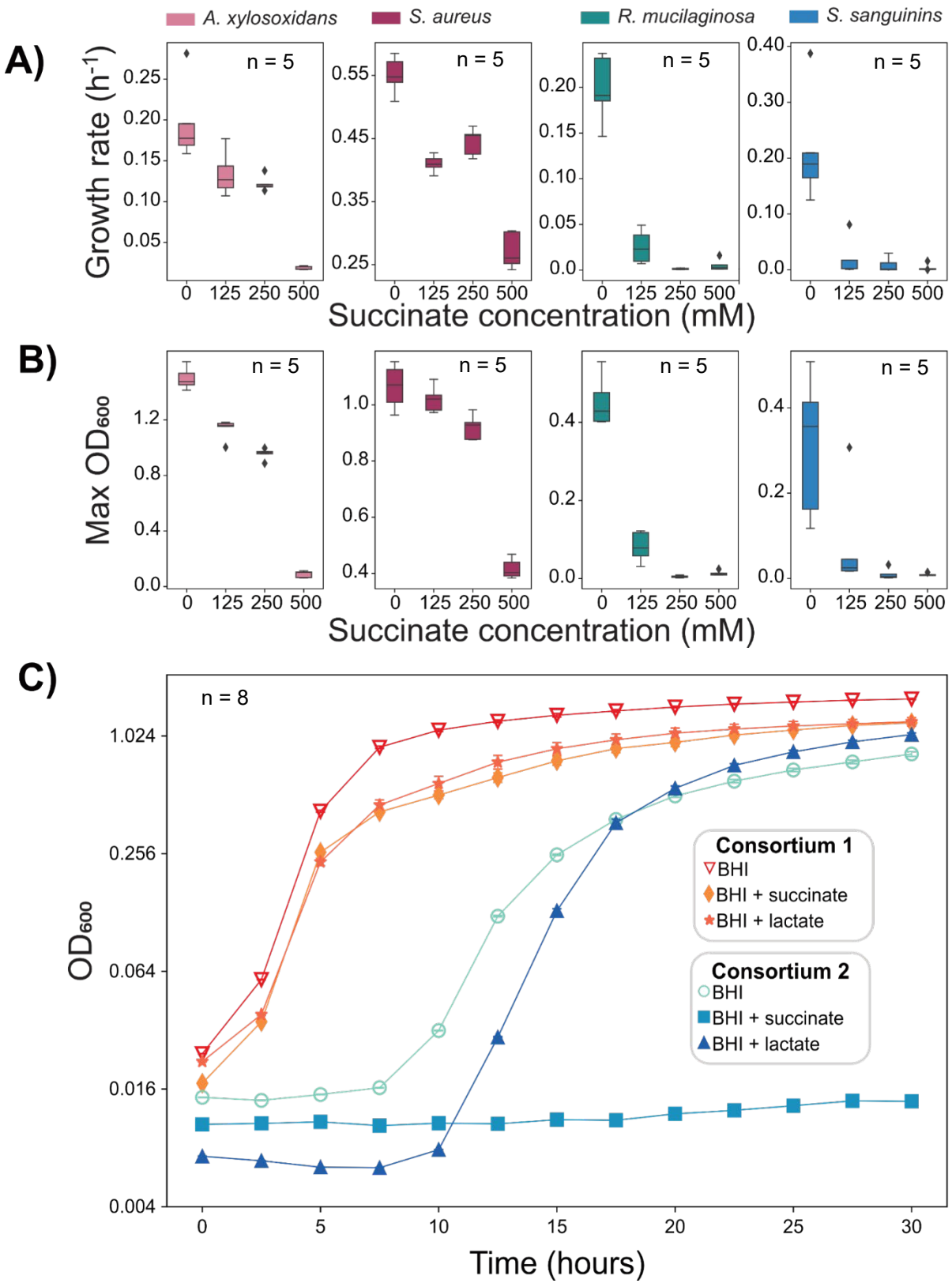
A)
A. xylosoxidans
S. aureus
R. mucilaginosa
S. sanguinins
Growth rate (h-1)
n = 5
Succinate concentration (mM)
B)
Max OD600
C)
n = 8
OD600
Time (hours)
Consortium 1
BHI
BHI + succinate
BHI + lactate
Consortium 2
BHI
BHI + succinate
BHI + lactate

Succinate as a sole carbon source supported the growth of consortium 1 member *A. xylosoxidans* when cultured in M9 salts (Figure 2.4). A similar test with lactate showed that *A. xylosoxidans* was also able to use lactate as a sole carbon source, though its growth over 72 hours on succinate was logarithmic and reached OD_{600} = 0.8 whereas on lactate its growth was linear and reached OD_{600} = 0.2 (Figure 2.4). *A. xylosoxidans* was unable to grow in M9 when only formate or acetate was available (data not shown).

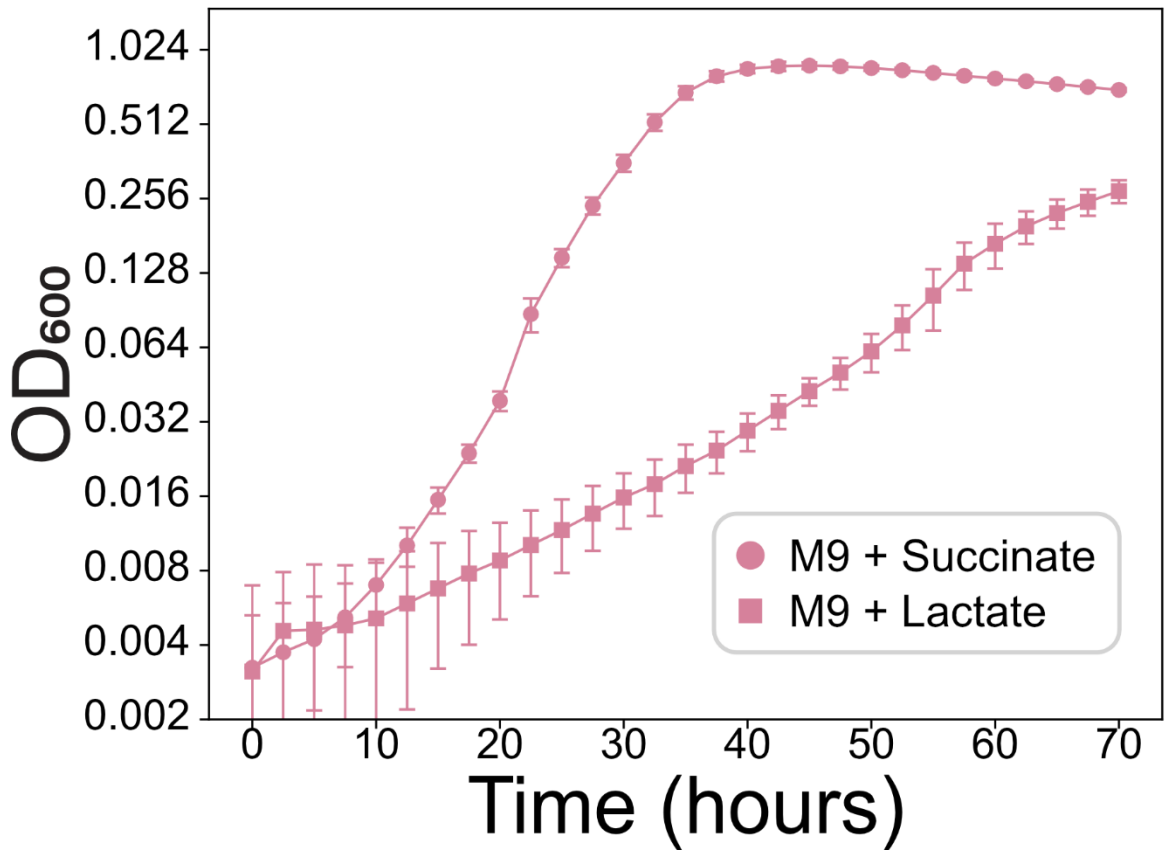

Figure 2.4: *A. xylosoxidans* can utilize succinate as a sole carbon source. Above is a growth curve of patient-isolated *A. xylosoxidans* grown in M9 salts supplemented with 250 mM succinate or lactate. Optical density was measured every half hour for 72 hours using 600 nm wavelength light.

A co-culture of consortium 1 members *A. xylosoxidans* and *S. aureus* was grown in BHI alone or BHI supplemented with succinate or lactate. The same culture conditions were used to monitor a co-culture of consortium 2 members *R. mucilaginosa* and *S. sanguinis*. Optical densities measured over 30 hours showed that both co-cultures increased in density when cultured in BHI or BHI+ lactate; however, only consortium 1 increased in optical density when cultured in BHI+ succinate while the optical density of consortium 2 remained near the time zero value of 0.01 (Figure 2.3C). Thus, the two consortia could likely co-exist in the presence of lactate but not succinate. In a separate experiment, high density overnight cultures were spun down and resuspended in fresh BHI with either a low concentration of succinate (10 mM) or a high concentration of succinate (250 mM). Optical densities were measured at time zero as well as at 12 hours. Consortium 1 increased in optical density as expected, while consortium 2 not only failed to grow but actually decreased, suggesting that 250 mM succinate is possibly bactericidal to consortium 2 (Table 2.1).

Table 2.1: Growth of consortium 1 and consortium 2 bacteria in low or high concentrations of succinate. High densities of bacteria were resuspended in fresh BHI with supplemental succinate and incubated at 37 degrees Celsius for 12 hours to asses growth via OD_{600}. N = 3, (+/-) is the standard deviation.

Growth in BHI with succinate after 12 hrs				
	10 mM succinate		250 mM succinate	
Rothia spp.	23%	+/- 1%	-6%	+/- 3%
Streptococcus spp.	41%	+/- 29%	-20%	+/- 3%
Achromobacter spp.	82%	+/- 5%	29%	+/- 28%
Staphylococcus spp.	2%	+/- 1%	2%	+/- 2%

2.2 Discussion

Concentrations of succinate in CF lungs are estimated to be ≈ 37 times higher than those in non-CF lungs, and up to 500 mM in the BAL from a mouse model that has a mutation to PTEN that prevents it from complexing with the CFTR (Riquelme et al., 2019). It has been shown that such a high concentration of succinate supports growth of *P. aeruginosa* (Riquelme et al., 2019) and, as shown herein, *A. xylosoxidans*. *In vitro* experiments validated the growth of *A. xylosoxidans* on succinate as a sole carbon source and the high tolerance of succinate by the other consortium 1 member *S. aureus*.

These results support the conceptual model shown in Figure 2.5. This model describes a cycle of succinate production by the CF epithelial cells, which selects for the growth of a succinate utilizing/tolerant community of bacteria (i.e., consortium 1). As this community grows, builds a biofilm and mucus accumulates into a purulent mass or a mucus plug, oxygen and succinate begin to be depleted locally. This depletion enables *S. sanguinis* and/or other consortium 2 bacteria to proliferate, producing lactate as a main byproduct of their metabolism. Inflammation of the local airway in response to these bacteria results in neutrophils infiltrating the mucus mass. Neutrophils that are trapped in this low oxygen environment produce even higher concentrations of lactate (Bensel et al., 2011). Upon resolution or expectoration of the mucus mass, the cycle begins again. A re-analysis of longitudinal datasets of sputum metagenomes from (C. Martin et al., 2023) shows that consortium 1 and 2 tend to correlate inversely with one another over time since seven of the eight longitudinal CF sputum metagenomic datasets had significant negative Spearman's correlation coefficients. (Supplementary Figures 2.4-10) One CF dataset had a positive Spearman's correlation coefficient but the p-value was not significant. (Supplementary Figure 2.11) The NonCF control dataset showed almost no presence of consortium 1, as expected (Supplementary Figure 2.12), thus lending support to the model in Figure 2.5. The NonCF control dataset did show the presence of consortium 2 bacteria, which makes sense since consortium 2 is made up of bacteria that are typical isolates of the human oral cavity.

In the context of the Climax and Attack Model of CF lung microbial ecology, consortium 1 is predicted to represent the Climax community that comprises resident microbes that can grow under high succinate concentrations; this community is likely dominated by a microbe that can utilize succinate to directly fuel its metabolism and growth. Consortium 2 is predicted to represent the Attack community, whose members rapidly increase in abundance as succinate is depleted and lung inflammation increases.

The importance of succinate to CF lung microbial ecology may be widespread in the CF community since high succinate concentrations in sputum are a direct consequence of CFTR mutation. Moreover, the GEMs analysis of the 29 most common microbes in CF lungs supports the ubiquity of microbial consortia that differ in their ability to metabolize or tolerate succinate (O'Toole et al., 2021). The conditions of CF sputum would favor microbes who can take up and/or tolerate succinate until the succinate has been depleted. Succinate depletion below the MIC for the oral cavity lactic acid bacteria, perhaps ≤125-250 mM, is likely associated with the establishment of biofilms and mucus plugs, whose high lactate concentrations and low oxygen concentrations would favor the oral cavity lactic acid bacteria. Thus, this work predicts that succession away from the succinate community (Climax) and toward the oral cavity lactate community (Attack) may be associated with mucus plugs and inflammation, both negative indicators of lung health. Previous *in vitro* studies have shown that using succinate as an adjuvant for ciprofloxacin and tobramycin can enhance killing of *Pseudomonas aeruginosa* (Bahamondez-Canas &

Smyth, 2018; Silva et al., 2020), likely due to succinate inducing bacterial growth, thus making the antibiotics more effective. However, it was also shown, in an *in vitro* experiment, that succinate showed cytotoxicity on human epithelial cells (Silva et al., 2020). A trial of succinate as an adjuvant for intravenous chloramphenicol in children with CF showed increased inhibition of “many important nonpseudomonal pathogens” when compared to oral administration with or without palmitate (Dickinson et al., 1988). Based on the results shown here, the “important nonpseudomonal pathogens” are likely to be from consortium 2. Future studies should seek to characterize the growth of more CF isolated strains of bacteria in the presence of succinate to validate the predictions of the GEMs. A longitudinal study of CF sputum that measures both the concentration of succinate in the samples as well as the composition of the microbial community would validate the predictions of Figure 2.5.

Figure 2.5: Model of succession from consortium 1 to consortium 2. Panel 1, high succinate concentrations in the mucus (provided by the CF lung epithelial cells) selects for consortium 1. Panel 2, then as consortium 1 proliferates and forms a mucus plug, succinate is locally depleted along with oxygen, allowing a consortium 2 microbe such as *Streptococcus* to grow and start producing lactate. Panel 3, neutrophil infiltration into a mucus plug further decreases oxygen, increases lactate and inflammation. Panel 4, low concentrations of succinate and the increased concentration of lactate allow for rapid proliferation of consortium 2 microbes until the plug is cleared and the cycle begins again.

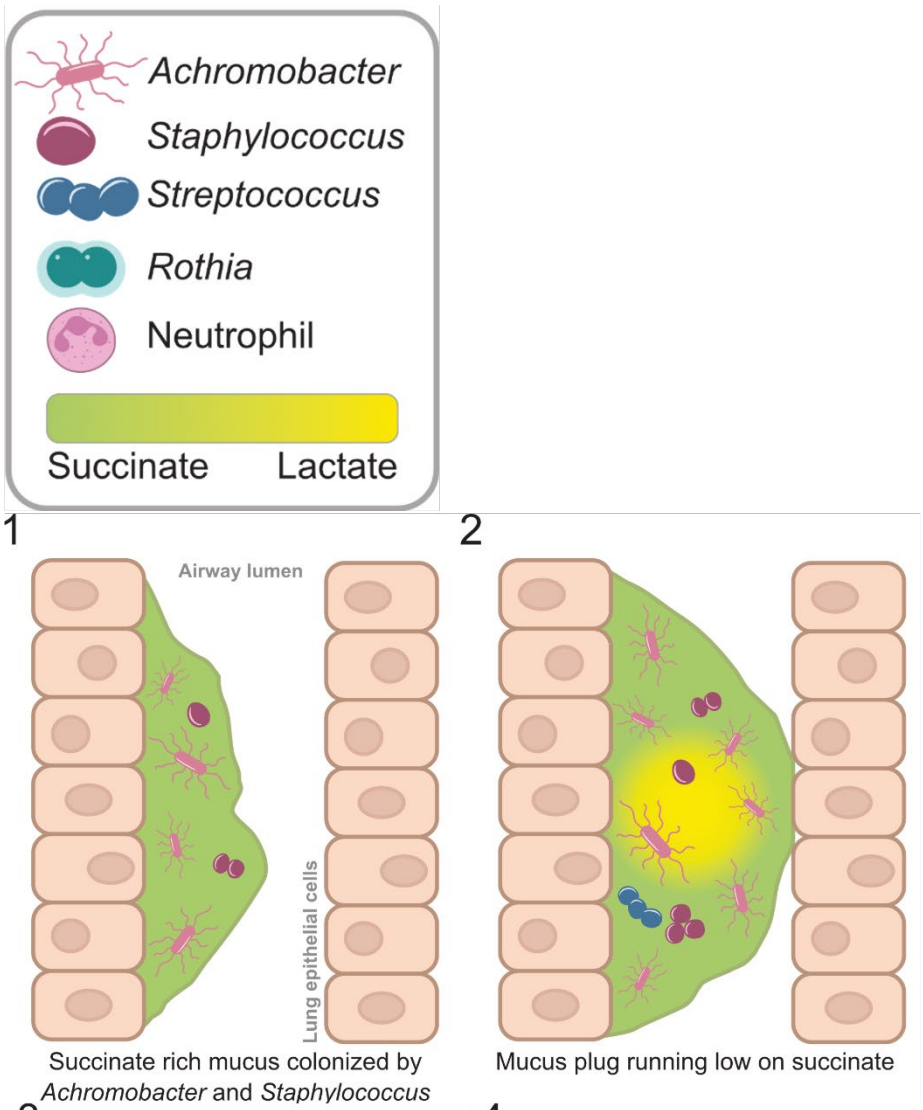
Achromobacter
Staphylococcus
Streptococcus
Rothia
Neutrophil
Succinate
Lactate
1
Airway lumen
Lung epithelial cells
Succinate rich mucus colonized by
Achromobacter and Staphylococcus
2
Mucus plug running low on succinate
3
Trapped neutrophil increasing
lactate concentration
4
High lactate and low succinate leads
to replacement by Consortium 2

2.3 Conclusion

Succinate concentrations in CF lungs likely favor the growth of *Achromobacter xylosoxidans*, while inhibiting sputum colonization by the oral cavity bacteria *Rothia mucilaginosa* and *Streptococcus sanguinis*. However, this inhibition is relieved when *A. xylosoxidans* depletes the succinate, which is predicted to lead to oscillations in the sputum microbial community from a succinate dependent/tolerant consortium (Climax community) to a succinate intolerant community of oral-derived opportunists (Attack community). Using these results and their predictions to improve our mechanistic understanding of CF lung microbial ecology has the potential to inform treatment decisions by helping physicians and scientists assess the efficacy of treatment, e.g., by using metabolomics and metagenomics to track pathogen metabolism and abundance over the course of treatment (D. Conrad et al., 2013a).

2.4 Methods

Metagenomics analysis

Metagenomes were selected from the Sequence Read Archive (SRA), by first exporting the list of accession numbers of all CF sputum metagenome entries. Then the list was sorted according to a list of randomly generated numbers. Read processing and taxonomic assignment was done using BV-BRC's (formerly PATRIC's) metagenomic analysis services rely on the Kraken2 algorithm (Olson et

al., 2023; Wood et al., 2019). Relative abundances of Bacteria were then used to make the hierarchically clustered heatmap of Spearman's correlation coefficients using SciPy's .corr method (Virtanen et al., 2020) to generate the correlation matrix and Seaborn's sns.clustermap function (Waskom, 2021) to generate the hierarchically clustered heatmap. Metagenomes that did not have any bacterial reads that mapped to the 13 most prevalent genera or at least 1000 fragments that were recruited to the bacterial clade by Kraken2 were discarded (some metagenomes only had fungal reads). Thirty CF sputum metagenomes were analyzed with 6 being discarded.

Longitudinal datasets

Nine longitudinal datasets of sputum metagenomes were re-analyzed from the Qiita repository (https://qiita.ucsd.edu/analysis/description/53908/) and published manuscript (Martin et al., 2023). Eight of those are from people with CF and one is from a non-CF patient. Relative abundances were extracted at the genus level with hits to each genus being taken at face value of the published analysis *i.e.* reads were not reassigned to taxonomy for this study. However, samples were normalized by subtracting the average number of hits for each genus found in the saline controls from their respective genus values found in the sputum samples. Relative abundances of the 13 most prevalent genera of bacteria of the CF lung, as shown in (Thornton et al., 2023), were then combined according to the two consortia and plotted over the day values provided by the authors. Meaning that if the sum of

consortium 1 added up to 10% of all of the bacterial reads and consortium 2 added up to 50% then the remaining 40% are bacterial reads that could not be classified down to the genus level or belong to bacterial genera outside of the 13 from (Thornton et al., 2023). Spearman's correlation coefficients and p-values were calculated for all nine longitudinal datasets using SciPy's spearmanr function.

Genome-Scale Metabolic Modeling in K-Base

Modeling the 29 most prevalent bacterial species in the CF lung. Metagenomes from 73 CF sputum samples were randomly selected from the ≈2700 available in the Sequence Read Archive using BV-BRC's microbiome analysis service. The results were sorted according to the 13 genera from (Thornton et al., 2023). Species from each genus with a z-score above 2 or a prevalence over 25% were selected to make GEMs. For each species selected, the Refseq genome was uploaded to K-Base for creating metabolic models and FBAs, with gaps filled on LB. Gap filling is the process of adding enzymes not annotated in the genome but are required to grow on a given media. LB was the most complex media available on K-Base at the time of the analysis and could support the growth of all of the bacteria used in the *in vitro* assays performed in the study (though the growth was very poor for *S. sanguinis* & *R.* mucilaginosa). This resulted in the production of 29 distinct metabolic models. Flux values for the succinate reactions and oxygen import reactions for each species were used to calculate a z-score matrix. That z-score

matrix was then used to generate a hierarchically clustered heatmap of Spearman's correlation coefficients.

Strain isolation using alginate beads as analogs for CF mucus plugs:

Artificial sputum medium (Quinn et al., 2015b), inoculated directly with one sample of the patient's sputum (provided prior to hospitalization), was solidified into roughly 2 cm diameter oblong beads by adding 1.5% sodium alginate, then pouring the mixture into a mold made of 2% agar with 1% calcium chloride. The calcium chloride ionically crosslinked the alginate to form a calcium alginate hydrogel. Once the mold was filled, the entire mold was submerged, at least 5 cm below the surface, in a bath of sterile 1% calcium chloride in water. Once the alginate beads solidified, the beads were separated and each bead was placed into an individual well within a 12 well plate. Each bead was suspended in RPMI cell culture media supplemented with 10% Fetal Bovine Serum (FBS) and incubated for 96 hours at 37 degrees Celsius with 5% CO_2; RPMI and FBS were replaced daily. At 96 hours the beads were transferred to a sterile mortar and pestle for mechanical disruption. Disrupted beads were then recovered into SM buffer and serial 10-fold dilutions were performed. A 100 uL aliquot of the 10^{-6} dilution was plated on 15 cm LB agar plates. Distinct colony morphologies were streak purified 3 times before choosing a single

colony for genomic DNA extraction and whole-genome sequencing to validate taxonomic assignment by colony morphology.

Experimental Determination of Growth Phenotypes for Model Validation

Brain and Heart Infusion media (BHI) (Difco) was used to grow the isolated strains because it supported growth of all strains used in this paper. Note that LB (the most complex digital media available), which was used for GEMs, did not support efficient growth of *R. mucilaginosa* or *S. sanguinis* and thus was not used for testing *in vitro* growth of the two consortia. Cells from overnight cultures of each bacterial strain were washed 4 times in M9 salts then starved overnight before being diluted 1:250 into the media and loaded into flat-bottom clear polystyrene 96-well plates. Growth curves were carried out by measuring optical densities at 600 nm on a Versamax Absorbance Microplate reader. Plates were incubated at 37 degrees Celsius with optical density readings every 30 minutes; plates were shaken for 30 seconds of the 30-minute interval, before every reading. Growth rates and maximum optical densities were calculated using the AMiGA analysis software, version 2.0.0 - 2021-04-21 (Midani et al., 2021). Each growth rate or max OD_{600} in Figure 2.2 A or B represents an average of 5 biological replicates (new colony used for inoculum on a new day) where each biological replicate included 5 technical replicates (replicate wells inoculated with the same colony).

Chapter 2, in part, is currently being prepared for submission for publication of the material. Canto-Encalada, Gabriela; Julazadeh, Hana; Bailey, Barbara A.; Rohwer, Forest; Zúñiga, Cristal. The dissertation author was the primary researcher and author of this material.

CHAPTER 3 Novel receptor binding domains fused to the R2 pyocin tail fiber kill target bacteria.

Tailocins are intact tail structure remnants of defective prophages that can no longer form a capsid (Ghequire & De Mot, 2015). These tail structures (contractile tail, baseplate and tail fibers), encoded by bacterial genomes, can still bind to and kill bacteria in releasing the kinetic energy stored in the tail to insert a pore in the bacterial membrane, causing membrane depolarization and lysis. Indeed, tailocins have been co-opted by bacteria to use against competing strains or species (Ghequire & De Mot, 2015).

Tailocins show therapeutic potential as novel bactericidal particles because they bind to and kill their bacterial targets very specifically. One advantage to pursuing tailocins as bactericidal agents is that they do not have genomes, thus cannot transfer genes to, or integrate into, genomes of the target bacteria. In addition, tailocins cannot reproduce, and each tailocin can at maximum kill one bacterial cell before it becomes inert, making it feasible to control the dose. Engineering tailocins for therapeutic purposes is accomplished using standard techniques to modify host target specificity, (i.e., the receptor binding domains (RBDs) of an existing and well-studied tail “chassis.” One such system is called Avidocin, from Pylum Biosciences, which uses the R2 pyocin (tailocin) found in *Pseudomonas aeruginosa* as a chassis whose RBD can be modified using several techniques (D. W. Jr. Martin et al., 2010; Williams et al., 2008). The addition of the

tailspike from Φ V10 as the new receptor binding domain allowed the Avidocin (modified R2 pyocin) to bind to and kill *Escherichia coli* O157:H7 (Ritchie et al., 2011; Scholl et al., 2009). Hypothetically, as long as an RBD is compatible with the R2 tail fiber and confers bacterial binding, then the modified R2 pyocin should be able to kill the new target strain of bacteria.

3.1 Results

Using the same tailocin modification system as the Pylum Biosciences Avidocin construct, two novel modified tailocins were engineered (Figure 3.1A). Both novel tailocins produced protein bands of the expected molecular weight of ≈100 kilodaltons when run on SDS PAGE (Figure 3.1B). The first tailocin, MobyWanKenobi, was produced by fusing the R2 tail fiber with the tailspike of Φ-Moby. Φ-Moby is a myophage (contractile tailed phage) that infects *Stenotrophomonas maltophilia*, an opportunistic pathogen found in immunocompromised patients that is often highly antimicrobial resistant. The R2 tail fiber/Moby tailspike fusion allowed MobyWanKenobi to kill stationary phase cells of a strain of *Stenotrophomonas maltophilia* isolated from a cystic fibrosis patient's sputum (Figure 3.2B). Cystic fibrosis bacterial isolates are often highly antimicrobial resistant due to the near constant antibiotic treatments administered to people with CF, and the ability of non-growing cells in the biofilms of purulent mucus masses to persist past the biological half-life of the administered antibiotic.

Figure 3.1: A, schematics depicting R2 and the modified forms. Left: R2 chassis; middle: MobiWanKenobi; right: John Henry. B, An SDS-PAGE image of the MobyWanKenobi and John Henry tailocins compared with Avidocin as a control with molecular weights expected to be greater than or equal to 100 kilo Daltons as shown in (Scholl et al., 2009). Protein bands were visualized using Sypro Ruby. *, putative tailocin multimer.

A

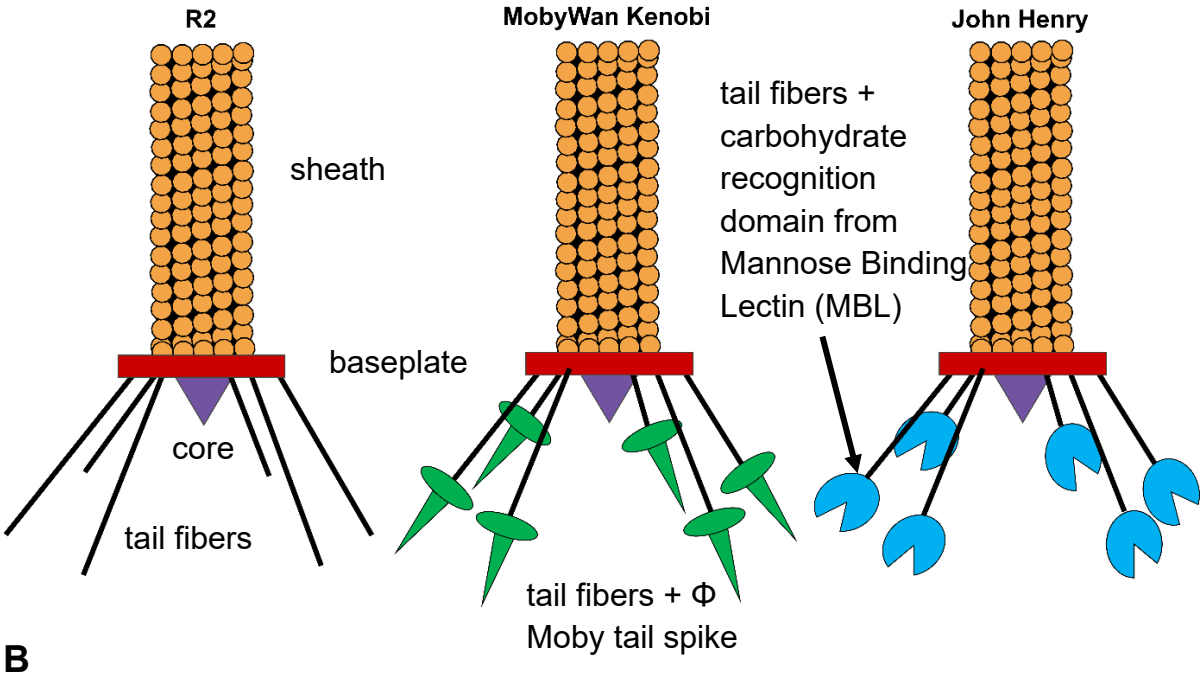
R2
MobyWan Kenobi
John Henry
sheath
baseplate
core
tail fibers
tail fibers + carbohydrate recognition domain from Mannose Binding Lectin (MBL)
tail fibers + Φ
Moby tail spike

B

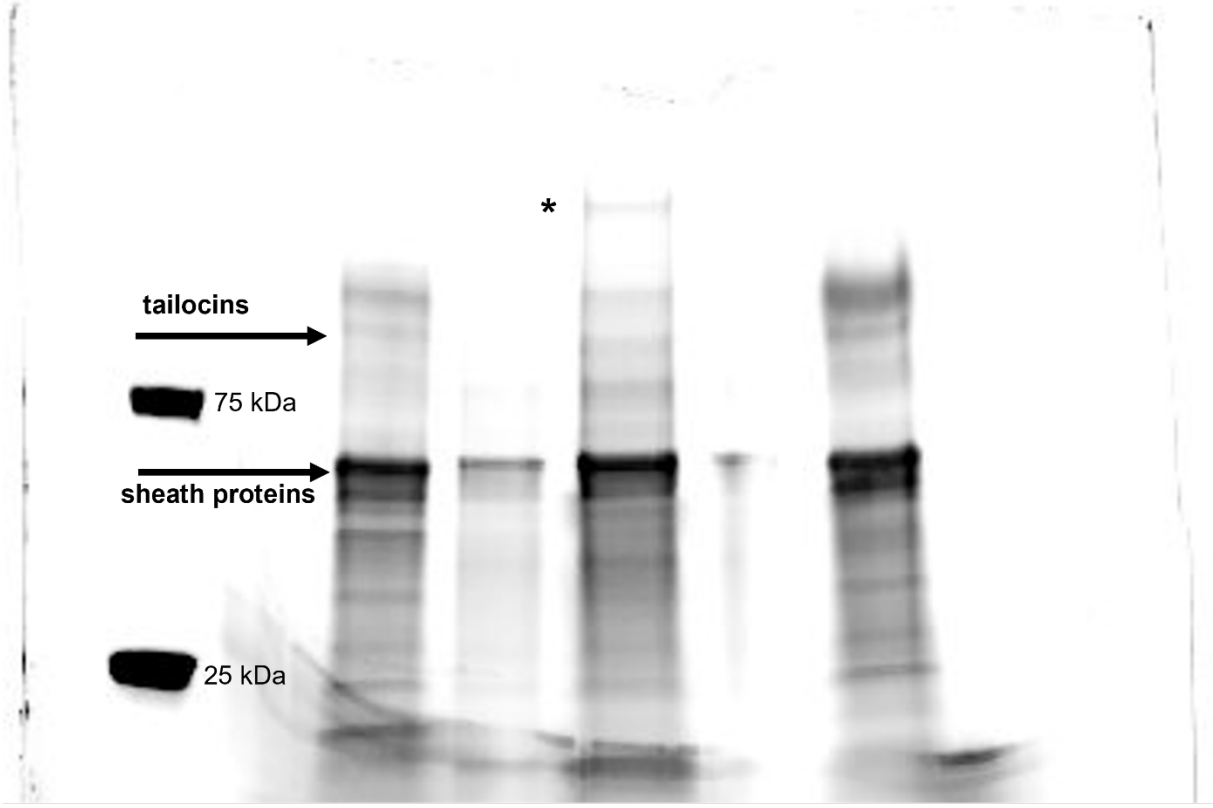
*
tailocins
75 kDa
sheath proteins
25 kDa
ladder
Avidocin
spill over
MobyWanKenobi
John Henry
spill over

Treating a 100 uL cell suspension of *E. coli* O157:H7 or the *S. maltophilia* CF isolate with 100 uL of MobyWanKenobi (≈1.3 x 10^8 tailocins, calculated using equation 1) for 30 minutes showed that this tailocin is specific for S. *maltophilia* (Figure 3.2). The abundance of *S. maltophilia,* measured as Colony Forming Units (CFU), was over 3-fold lower than an carbon free M9 salts solution control (Figure 3.2B) whereas the abundance of *E. coli* O157:H7 was not reduced compared to the carbon free M9 salts solution control (Figure 3.2A). Moreover, the Avidocin tailocin (Scholl et al., 2009) was able to reduce *E. coli* O157:H7 CFU several orders of magnitude (Figure 3.2A) whereas it did not affect CFU abundances of *S. maltophilia* (Figure 3.2B).

Figure 3.2: The tailocins MobyWanKenobi and Avidocin specifically target *E. coli* O157:H7 and S. maltophilia, respectively. Panel A shows total bacterial abundance of a suspension of *E. coli* serogroup O157:H7 after 25 minutes of treatment with carbon free M9 salts solution, MobyWanKenobi or Avidocin. Panel B shows total bacterial abundance of a suspension of *S. maltophilia* (CF isolate) after 25 minutes of treatment.

A

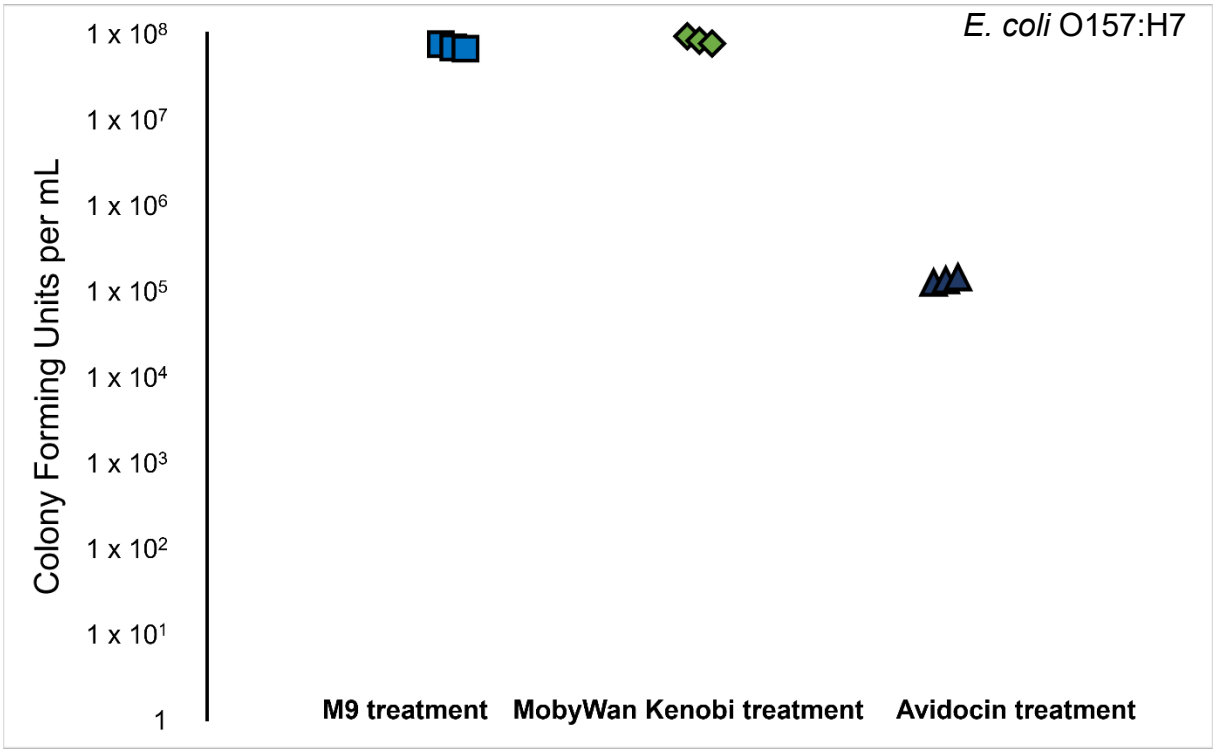
E. coli O157:H7
1 x 10^8
1 x 10^7
1 x 10^6
1 x 10^5
1 x 10^4
1 x 10^3
1 x 10^2
1 x 10^1
1
Colony Forming Units per mL
M9 treatment
MobyWan Kenobi treatment
Avidocin treatment

B

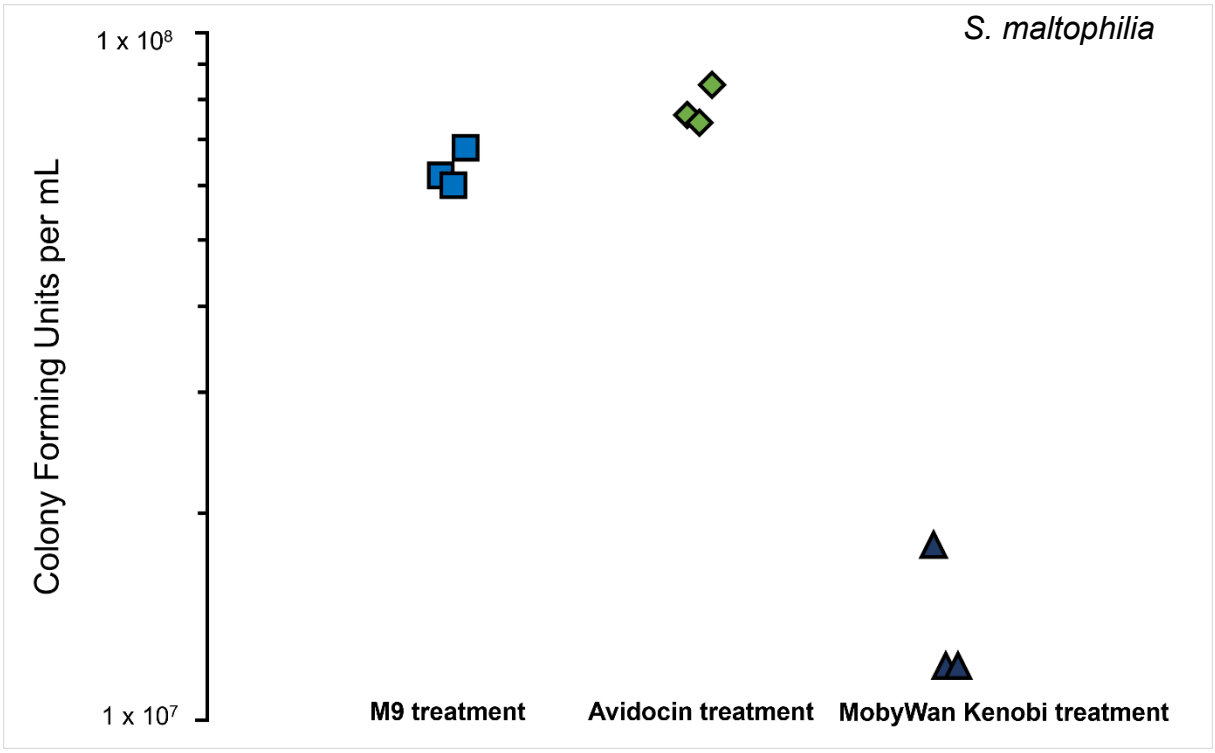
S. maltophilia
1 x 10^8
1 x 10^7
Colony Forming Units per mL
M9 treatment
Avidocin treatment
MobyWan Kenobi treatment

The second tailocin, John Henry, was produced by fusing the R2 tail fiber with the carbohydrate recognition domain of human Mannose-Binding Lectin (MBL). MBL is part of the immune system's complement cascade that recognizes the bacterial cell surface and recruits other proteins in the membrane attack complex. MBL binds to N-acetylglucosamine (NAG), a Pathogen Associated Molecular Pattern (PAMP), that is present in both the bacterial cell membrane and the cell wall, thus allowing MBL to recognize both gram-positive and gram-negative bacteria lacking an S-layer. Fusing MBL with the R2 pyocin tail fiber may have enabled binding to a broader spectrum of bacterial cell surfaces, as evidenced by its ability to kill *Serratia odorifera* (gram-negative) and *Staphylococcus aureus* (gram-positive), both of which were isolated from cystic fibrosis sputum.

Nine hundred microliters of high density (> 1 OD_{600}) *Serratia odorifera* and *Staphylococcus aureus* cells suspended in SM buffer (100 mM NaCl, 8 mM $MgSO_4$ & 50 mM Tris HCl pH 7.5) were incubated with 100 uL of a John Henry lysate, that had also been buffer exchanged into SM buffer, for 30 minutes, the CFU count of each species was reduced by the same amount ≈$2.3x10^9$ CFUs per mL (Figure 3.3). The bacteria were suspended in SM buffer to prevent their rapid growth from confounding the observations of killing since both bacteria have generation times less than the tailocin incubation time of 30 minutes described in (Scholl et al., 2009). Tailocins are only bactericidal, not bacteriostatic, meaning once a tailocin killing event is complete the surviving bacteria will continue to grow. The last filtrate from the buffer exchange process was used as the buffer control to ensure no contaminating antibiotics or

mitomycin C from the tailocin production process remained active in the final lysate (see Methods). The tailocin treatment conditions from Figure 3.3 were observed every 30 minutes for a total of two hours, which showed complete recovery of the bacterial population to pre-treatment levels at the two-hour timepoint (Supplementary Figure 3.1). Since these were stationary phase cells suspended in a nutrient free SM buffer this is what one would expect if the observed killing were caused by a tailocin, since tailocins are one-shot contractile structures which become inert once triggered. Meaning the contents of the lysed cells were the only nutrients available for the cells to use for growth, thus explaining the two-hour recovery time when it would have taken less than 30 minutes to recover in rich media. This is similar to observations made in (González-Pastor et al., 2003) were *B. subtilis* was shown to cannibalize lysed cells during spore formation. Identical tailocins were also engineered to be produced by *Serratia odorifera* and *Achromobacter xylosoxidans*. When produced and isolated from these two bacteria, the tailocin resulted in a similar reduction in CFU of *Staphylococcus aureus* (not measured in case of *Serratia odorifera*; Figure 3.4).

Figure 3.3: Tailocin John Henry reduces cfu of gram-positive and gram-negative bacteria by the same amount (2.3 x 10^9 CFU per mL). Panel A shows suspensions of *Serratia odorifera* treated with the same amount of the John Henry tailocin or the last filtrate from the buffer exchange process. Panel B shows suspensions of *Staphylococcus aureus* treated with the same amount of the John Henry tailocin or the last filtrate from the buffer exchange process.

A


Serratia odorifera
8 x 10⁹
7 x 10⁹
6 x 10⁹
5 x 10⁹
4 x 10⁹
3 x 10⁹
2 x 10⁹
1 x 10⁹
Colony Forming Units per mL
Before John Henry
After John Henry
After buffer control

B

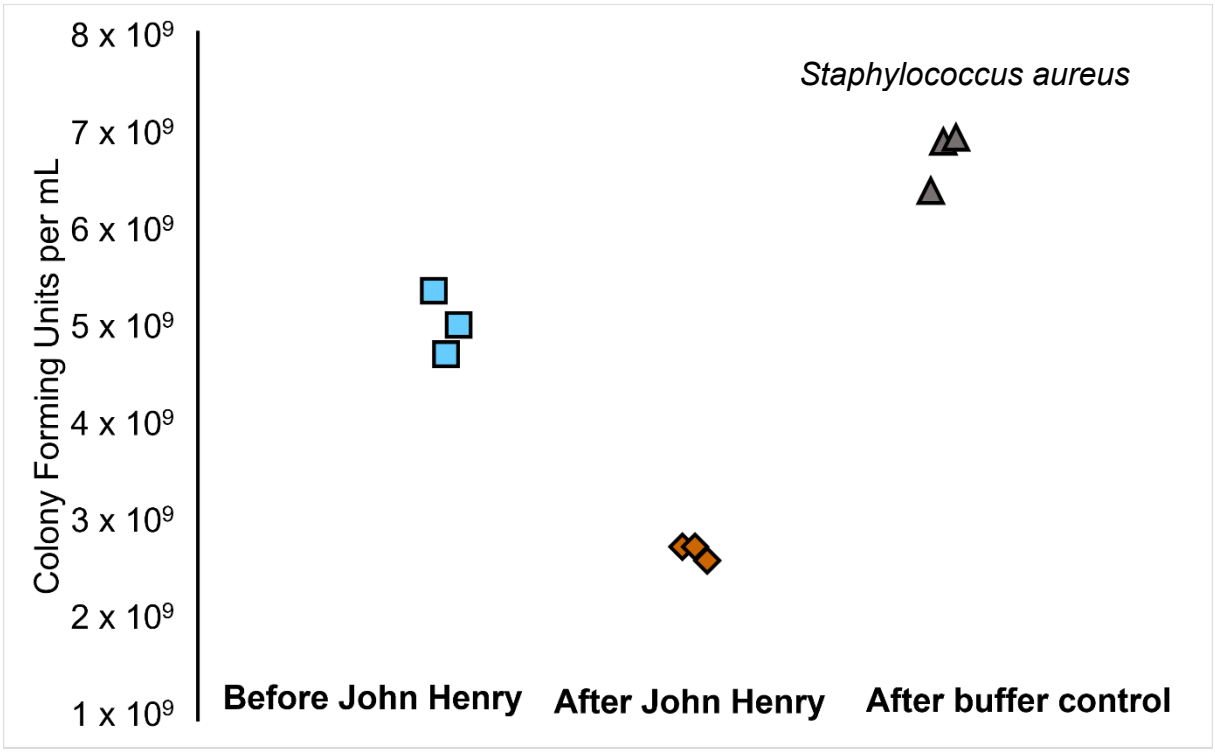
Staphylococcus aureus
8 x 10⁹
7 x 10⁹
6 x 10⁹
5 x 10⁹
4 x 10⁹
3 x 10⁹
2 x 10⁹
1 x 10⁹
Colony Forming Units per mL
Before John Henry
After John Henry
After buffer control

Figure 3.4: John Henry tailocins produced using a different genetic construct in two different host bacteria (panel A: *Serratia odorifera*; panel B: *Achromobacter xylosoxidans*) were active against *Staphylococcus aureus*. These tailocins were induced using IPTG and arabinose rather than mitomycin C; the genetic construct did not induce lysis during production so the lysates were produced via sonication of the bacterial pellet after induction. The lysates were then cleaned of any residual antibiotics via ultrafiltration/buffer exchange in the same manner as for the experiment shown in Figure 3.3

A

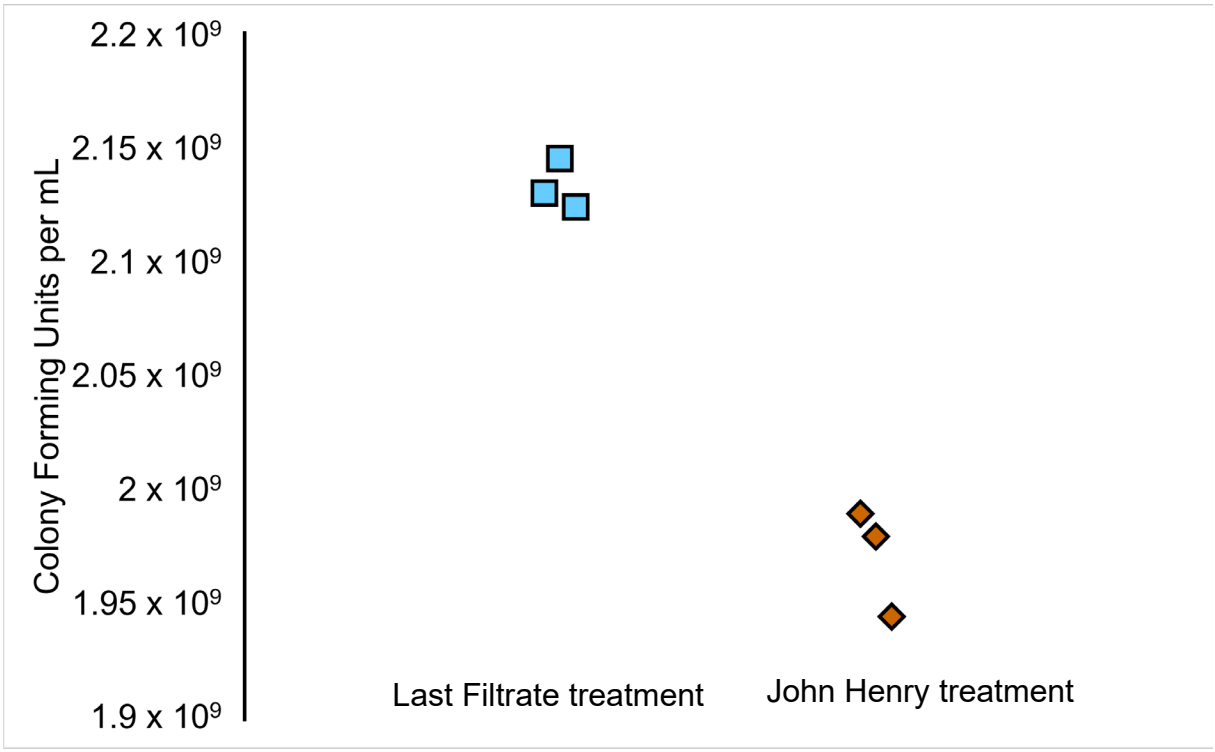
2.2 x 10^9
2.15 x 10^9
2.1 x 10^9
2.05 x 10^9
2 x 10^9
1.95 x 10^9
1.9 x 10^9
Colony Forming Units per mL
Last Filtrate treatment
John Henry treatment

B


2.8 x 10^8
2.6 x 10^8
2.4 x 10^8
2.2 x 10^8
2.0 x 10^8
1.8 x 10^8
1.6 x 10^8
1.4 x 10^8
1.2 x 10^8
1.0 x 10^8
Colony Forming Units per mL
Last Filtrate treatment
John Henry treatment

Determining the number of active tailocin particles in a given lysate is dependent on knowing the number of cells in a suspension before adding tailocins to that suspension. This is because there is a negative natural logarithmic relationship between the number of surviving target cells and the ratio of tailocins to the number of target cells before treatment, thus the number of tailocins in a given lysate is calculated using equation 1:

$$M = -lnS$$ Equation 1.

where M represents the number of tailocins per cell and S represents the percent surviving cells (Williams et al., 2008). This indicates that in order to reduce the number of cells that survive a single treatment requires that the tailocin dose must increase, but with dramatically diminishing returns as the value of M increases. This can be observed by treating multiple known concentrations of bacteria with the same amount of the same tailocin lysate to demonstrate the logarithmic decay in killing efficiency predicted by equation 1. MobyWan Kenobi closely matched the values of S predicted by equation 1 when observed by treating three different concentrations of stationary phase bacteria resuspended in M9 salts solution (undiluted, 1:4 dilution and 1:10 dilution), alongside Avidocin as a positive control (Figure 3.5). Even though there were 1.6 MobyWan Kenobi for each *Stenotrophomonas* only ≈88% of the bacteria were killed.

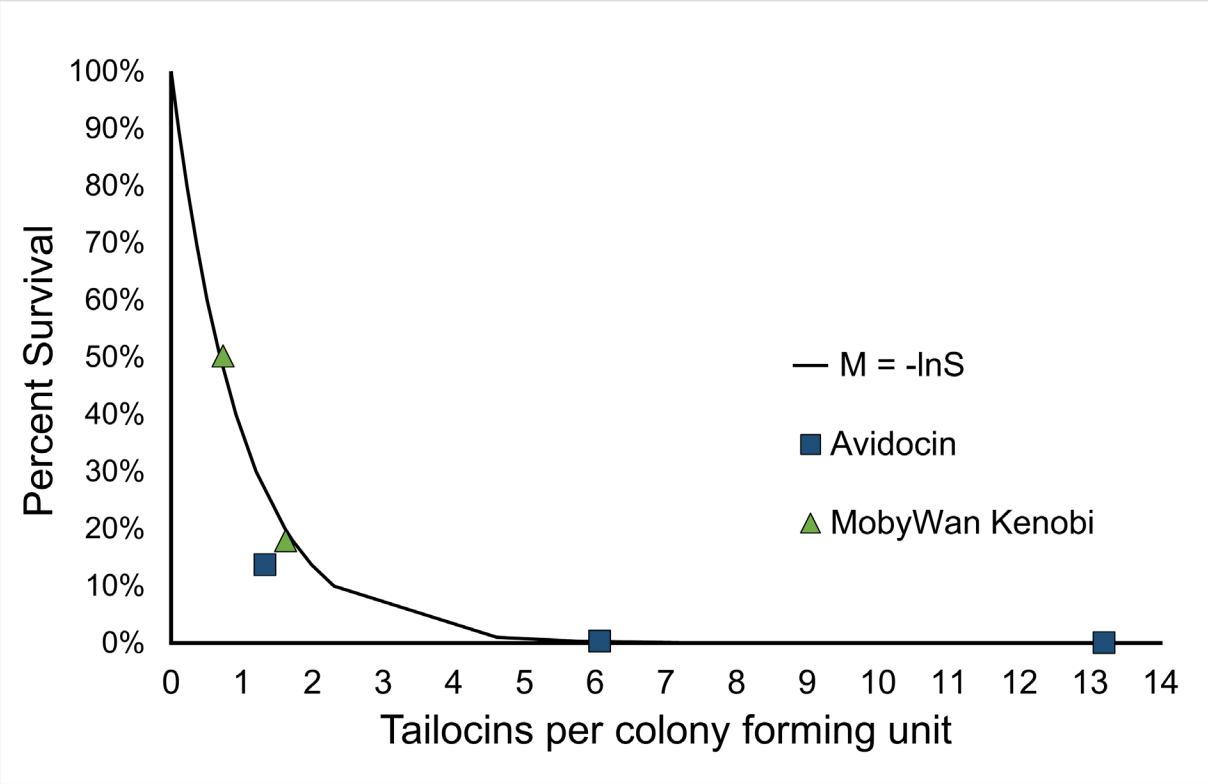

Figure 3.5: MobyWan Kenobi and Avidocin closely match the values predicted by equation one. This graph shows the percent of surviving bacteria (S) as a function of the number of tailocins per bacterial cell (M). The same volume of the same lysate was added at different dilutions of the same bacterial suspension in M9 salt solution. An error during plating led to missing observations for the undiluted bacterial concentration for MobyWan Kenobi. Avidocin lysate was added to *E. coli* O157:H7 (Undiluted was 1.1 x 10^8 CFU per mL), while MobyWan Kenobi was added to *Stenotrophomonas maltophilia* (Undiluted was 6.3 x 10^8 CFU per mL).

3.2 Discussion

A possible therapeutic use of tailocins may be the administration of successive tailocin treatments at doses that would yield predicted values of M below one, while a bacteriostatic antibiotic is co-administered to keep the bacteria from rebounding between treatments. That treatment modality may allow for the most efficient use of

tailocins as an antimicrobial. One challenge of such a treatment strategy is that sudden lysis of a large number of bacterial cells can cause inflammation, as triggered by the sudden release of bacterial cell debris (e.g., lipopolysaccharide or LPS, lipoteichoic acid or LTA and peptidoglycan) (Luo & Song, 2021; Venkataranganayaka Abhilasha & Kedihithlu Marathe, 2021). In light of this risk two dual purpose tailocins were designed with enzymes as their receptor binding domains. The first such tailocin was designed as a fusion between the human acyloxyacyl hydrolase enzyme and the R2 tail fiber. Acyloxyacyl hydrolase is an enzyme expressed in macrophages that degrades LPS such that it is no longer recognized as a PAMP by the innate immune system (Pohlman et al., 1987). The second such tailocin was designed with lysozyme fused to the R2 tail fiber. Lysozyme is a peptidoglycan-degrading enzyme, and the engineered version in this work was hen's egg lysozyme (Abraham, 1939; Hewitt, 1931; Ridley, 1928).

If these two dual purpose tailocins were administered together they would be able to bind to and kill gram-negative and gram-positive bacteria while also degrading the LPS and peptidoglycan produced by bacterial lysis, before they reach the bloodstream. These tailocins would also provide a single tailocin the ability to kill more than one bacteria, since even after the kinetic energy of the contractile tail is spent, the enzymes would still be active. Preliminary experiments to engineer these tailocins in *P. aeruginosa* resulted in the production of proteins of the expected molecular weight (Figure 3.6) but no killing activity, likely due to being prematurely triggered by the bacterial cells used to produce them. Growth of the production strain

was also poor and often resulted in premature lysis. Future work with these tailocins could include moving production from bacteria to a eukaryotic host such as yeast so that the enzyme tailocins can be efficiently produced in the absence of their substrates LPS and peptidoglycan.

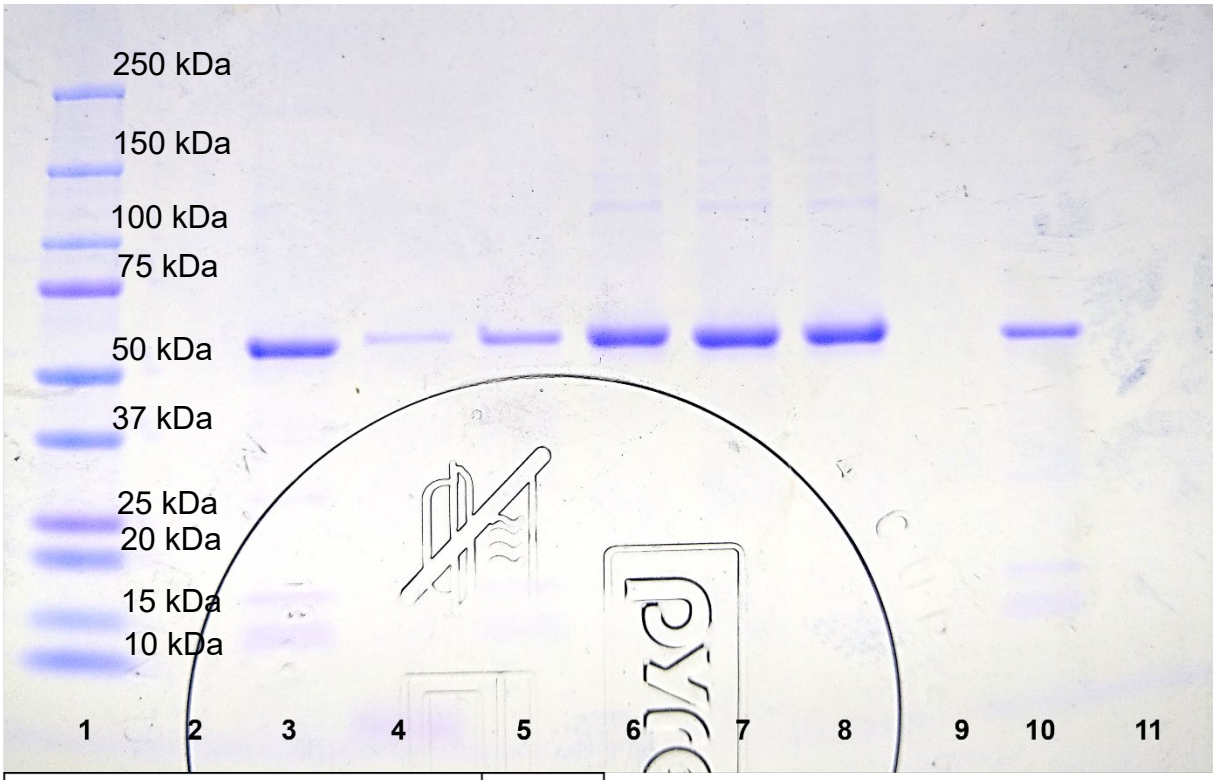

Lysate	Lane
Ladder	1
MΔR strain	3
MobyWan Kenobi	6
MΔR strain + DG203_lysozyme	7
MΔR strain + DG203_acyloxyacyl hydrolase	8
Unrelated	4, 5, 10
Empty	2, 9, 11

Figure 3.6: SDS-PAGE of tailocin lysates produced in *Pseudomonas aeruginosa* strain MΔR stained with Coomassie Blue. Expected molecular weight of fully assembled tailocins is > 100 kDa, sheath proteins expected at > 50 kDa.

3.3 Conclusion

The R2 pyocin has demonstrated its versatility as an engineerable protein construct with potential as a vehicle for the generation of both specific and broad-spectrum antibiotics. This is evident in the successful production of two new tailocins, MobyWanKenobi and John Henry. MobyWanKenobi specifically kills *S. maltophilia* while John Henry appears to have a broader spectrum according to the results in this work. Although the extent of the target range of John Henry is not yet known, the fact that it killed both a gram negative and a gram positive in the preliminary experiments is indicative of a broad spectrum tailocin. This work adds two engineered tailocins to the list of potential solutions to treat antibiotic resistant infections.

3.4 Methods

Vector construction

Shuttle vectors with the R2 tail-fiber/novel RBD fusion were constructed using Gibson assembly to insert amplicons of the novel RBDs into the DG203 shuttle vector as described in (D. W. Jr. Martin et al., 2010; Scholl, 2017; Scholl et al., 2009). The DG203 shuttle vector provided by Pylum Biosciences contained a truncated copy of the R2 pyocin tail fiber fused to a truncated ΦV10 tailspike under a Ptac promoter and a gentamycin resistance cassette. The ΦV10 tailspike was removed using restriction enzyme digest with HindIII and XbaI so that new RBDs could be added to

the truncated tail fiber sequence via Gibson assembly. Φ Moby tailspike was amplified directly from a phage lysate (Vicary et al., 2020) while the carbohydrate recognition domain of MBL was codon optimized for expression in *P. aeruginosa* and synthesized by GenScript (genscript.com). The carbohydrate recognition domain of MBL was then amplified from the plasmid containing the codon-optimized sequence provided by GenScript.

Transformation

Circularized vectors were transformed into DH10Beta via Polyethylene Glycol (PEG), according to (Chung et al., 1989), for storage and plasmid production. Plasmids were extracted from the storage strain using Zymo Research BAC DNA Miniprep kit, and transformed into strain MΔR (Scholl et al., 2009), whose genome contains the R2 tailocin with the tail fiber gene knocked out, and thus does not produce a high molecular weight band characteristic of the fully assembled tailocin after induction with mitomycin C.

Tailocin production

MobyWanKenobi was produced according to the protocol in (Scholl et al., 2009), then concentrated via PEG precipitation according to the protocol in (Kandel et al., 2020). Briefly, tailocin production cells were grown to OD_{600} 0.25 before adding

mitomycin C to induce tailocin production, cells were incubated and shaken until the culture completely lysed. Then DNAse and RNAse were added to remove genomic and ribosomal debris as well as lower the viscosity of the lysate. Then 10% PEG (w/v) and NaCl to 1 M were added to the lysate, then placed on a rocker at 4 °C for 16 hours before precipitating the tailocins via centrifugation at 16,000 g for 1 hour (adding Coomassie blue will make the pellet much easier to find). Protein pellets were then resuspended in carbon free M9 salts solution and stored at 4 °C. John Henry tailocin was produced and concentrated as described above but extra care was taken to ensure no residual antibiotics or mitomycin C would contaminate the resulting preparation, since there was not a negative control available for this broad spectrum tailocin. For this reason, John Henry tailocins were resuspended after precipitation, then the resuspension buffer was exchanged by ultrafiltration using Amicon Ultra-15 centrifugal filter units, Amicon's 50 mL centrifuge tube format, with a 100,000 molecular weight cutoff filter. The upper reservoir was loaded with the resuspended tailocins then filled to the maximum volume (15 mL) with fresh SM buffer (100 mM NaCl, 8 mM $MgSO_4$ & 50 mM Tris HCl pH 7.5). This assembly was centrifuged at 2,000 g until 1 mL or less remained in the upper reservoir. Flow through in the lower reservoir was discarded, and the upper reservoir was refilled. This was repeated for a total of 5 iterations, to ensure that no residual antibiotics or mitomycin C were present. Production strains can be found in Supplementary table 3.2.

Tailocin killing assays

MobyWanKenobi particles were added to stationary phase cells, from *S. maltophilia* or *E. coli* O157:H7, suspended in carbon free M9 salts solution. Avidocin particles were produced and added to the bacterial suspensions to act as both a positive control for tailocin killing of *E. coli* O157:H7 as well as negative control for killing of *S. maltophilia*. Mixtures of tailocins and cells were placed on a rocker for 30 minutes before quantifying bacterial abundances via colony forming units. John Henry tailocins suspended in SM buffer were added to stationary phase *S. odorifera* and *Staphylococcus aureus,* each of them also suspended in SM buffer, and allowed to rock for 2 hours while sampling to quantify bacterial abundances every 30 minutes.

Colony Forming Unit Assay: Total bacterial abundance was measured by sampling the mixture of tailocins and bacteria, diluting that sample (either in carbon free M9 salts solution or SM buffer) to 10^{-6}, then spreading 100 uL of that dilution on a 15 cm LB agar plate. Plates were incubated at 37 °C for at least 16 hours before counting the number of colonies on the plate.

SDS PAGE

A 10 uL volume of each isolated tailocin was mixed with 10 uL of 2x Laemmli buffer (without beta-mercaptoethanol) and loaded onto a BioRad pre-cast 4-20% tris glycine polyacrylamide gel. The gel was run for 36 minutes at 140 volts, variable amps in 1X BioRad tris glycine running buffer with SDS. Gels were stained with either

Coomassie Blue or Sypro Ruby. Coomassie Blue stained gels were imaged with a camera and a light box while Sypro Ruby gels were imaged using a Typhoon FLA 9000 gel imager. BioRad's Precision Plus Protein Standards Dual color, catalog number 161-0374, was used as the protein ladder.

Chapter 3, in part, is currently being prepared for submission for publication of the material. Julazadeh, Hana; Souza, Cole; Segall, Anca M.; Rohwer, Forest. The dissertation author was the primary researcher and author of this material.

APPENDIX

Supplementary Table 2.1: Kbase's digital LB, used for all FBAs in this dissertation.

compounds	name	formula	minFlux	maxFlux	concentration
cpd00001	H2O	H2O	-100	100	0.001
cpd00007	O2	O2	-100	100	0.001
cpd00009	Phosphate	HO4P	-100	100	0.001
cpd00018	AMP	C10H12N5O7P	-100	100	0.001
cpd00023	L-Glutamate	C5H8NO4	-100	100	0.001
cpd00027	D-Glucose	C6H12O6	-100	100	0.001
cpd00028	Heme	C34H30FeN4O4	-100	100	0.001
cpd00030	Mn2+	Mn	-100	100	0.001
cpd00033	Glycine	C2H5NO2	-100	100	0.001
cpd00034	Zn2+	Zn	-100	100	0.001
cpd00035	L-Alanine	C3H7NO2	-100	100	0.001
cpd00039	L-Lysine	C6H15N2O2	-100	100	0.001
cpd00041	L-Aspartate	C4H6NO4	-100	100	0.001
cpd00046	CMP	C9H12N3O8P	-100	100	0.001
cpd00048	Sulfate	O4S	-100	100	0.001
cpd00051	L-Arginine	C6H15N4O2	-100	100	0.001
cpd00054	L-Serine	C3H7NO3	-100	100	0.001
cpd00058	Cu2+	Cu	-100	100	0.001
cpd00060	L-Methionine	C5H11NO2S	-100	100	0.001
cpd00063	Ca2+	Ca	-100	100	0.001
cpd00065	L-Tryptophan	C11H12N2O2	-100	100	0.001
cpd00066	L-Phenylalanine	C9H11NO2	-100	100	0.001
cpd00067	H+	H	-100	100	0.001
cpd00069	L-Tyrosine	C9H11NO3	-100	100	0.001
cpd00084	L-Cysteine	C3H7NO2S	-100	100	0.001
cpd00091	UMP	C9H11N2O9P	-100	100	0.001
cpd00092	Uracil	C4H4N2O2	-100	100	0.001
cpd00099	Cl-	Cl	-100	100	0.001
cpd00107	L-Leucine	C6H13NO2	-100	100	0.001
cpd00119	L-Histidine	C6H9N3O2	-100	100	0.001
cpd00126	GMP	C10H12N5O8P	-100	100	0.001
cpd00129	L-Proline	C5H9NO2	-100	100	0.001
cpd00149	Co2+	Co	-100	100	0.001
cpd00156	L-Valine	C5H11NO2	-100	100	0.001
cpd00161	L-Threonine	C4H9NO3	-100	100	0.001
cpd00182	Adenosine	C10H13N5O4	-100	100	0.001
cpd00184	Thymidine	C10H14N2O5	-100	100	0.001
cpd00205	K+	K	-100	100	0.001
cpd00215	Pyridoxal	C8H9NO3	-100	100	0.001
cpd00218	Niacin	C6H4NO2	-100	100	0.001
cpd00219	Prephenate	C10H8O6	-100	100	0.001
cpd00220	Riboflavin	C17H19N4O6	-100	100	0.001
cpd00226	HYXN	C5H4N4O	-100	100	0.001
cpd00239	H2S	HS	-100	100	0.001
cpd00246	Inosine	C10H12N4O5	-100	100	0.001
cpd00249	Uridine	C9H12N2O6	-100	100	0.001
cpd00254	Mg	Mg	-100	100	0.001
cpd00311	Guanosine	C10H13N5O5	-100	100	0.001
cpd00322	L-Isoleucine	C6H13NO2	-100	100	0.001
cpd00381	L-Cystine	C6H12N2O4S2	-100	100	0.001
cpd00383	Shikimate	C7H9O5	-100	100	0.001
cpd00393	Folate	C19H17N7O6	-100	100	0.001
cpd00438	Deoxyadenosine	C10H13N5O3	-100	100	0.001
cpd00531	Hg2+	Hg	-100	100	0.001
cpd00541	Lipoate	C8H13O2S2	-100	100	0.001
cpd00644	PAN	C9H16NO5	-100	100	0.001
cpd00654	Deoxycytidine	C9H13N3O4	-100	100	0.001
cpd00793	Thiamine phosphate	C12H17N4O4PS	-100	100	0.001
cpd00971	Na+	Na	-100	100	0.001
cpd01012	Cd2+	Cd	-100	100	0.001
cpd01048	Arsenate	HAsO4	-100	100	0.001
cpd03424	Vitamin B12	C62H91CoN13O14PR	-100	100	0.001
cpd10515	Fe+2	Fe	-100	100	0.001
cpd10516	Fe+3	Fe	-100	100	0.001
cpd11595	chromate	H2CrO4	-100	100	0.001

SRA accession numbers for Figure 2.1: ERR5167243, SRR7080471, SRR3239231, SRR12184891, ERR3430918, ERR3431058, SRR12184517, ERR5167141, SRR10267762, SRR4081000, ERR3256635, SRR13305369, SRR13305279, SRR13304750, SRR13304842, SRR13304886, SRR13305134, SRR20794659, SRR4081102, SRR5162028, ERR5167369, ERR3431042, SRR12184331, ERR3430769, ERR3431054, SRR3238798, SRR5162018, SRR20794666, SRR12184534, SRR7080407, ERR3430826, SRR7080249, SRR13305028, SRR13305282, SRR13305324, ERR3430791, ERR3256615, SRR13305174, SRR3239237, SRR20794660, SRR12184601, SRR13305232, SRR8049279, ERR3430938, SRR12184633, SRR13305081, ERR3431069, SRR4081075, SRR13304822, SRR13304885, SRR13305254, SRR20794599, SRR13305294, SRR13305069, ERR3430765, ERR5167351, SRR13305154, SRR13305334, ERR5167350, SRR13305258, SRR8181700, SRR20794618, SRR12184620, ERR3256685, ERR5167242, ERR3430862, SRR20794684, ERR5167254, ERR5167387, ERR5167311, SRR13304824, SRR3238771, SRR12184366.

SRA accession numbers for Figure 2.2: SRR13305069, SRR13305174, SRR13305282, SRR8049279, ERR3256615, SRR13305294, SRR13305254, SRR13305232, SRR7080407, SRR13305081, SRR7080249, SRR13305028, SRR13305324, SRR20794599, SRR3239237, SRR12184534, SRR12184601, SRR20794666, SRR13304822, SRR13304885, SRR20794660, SRR4081075, SRR12184620, SRR13305154.

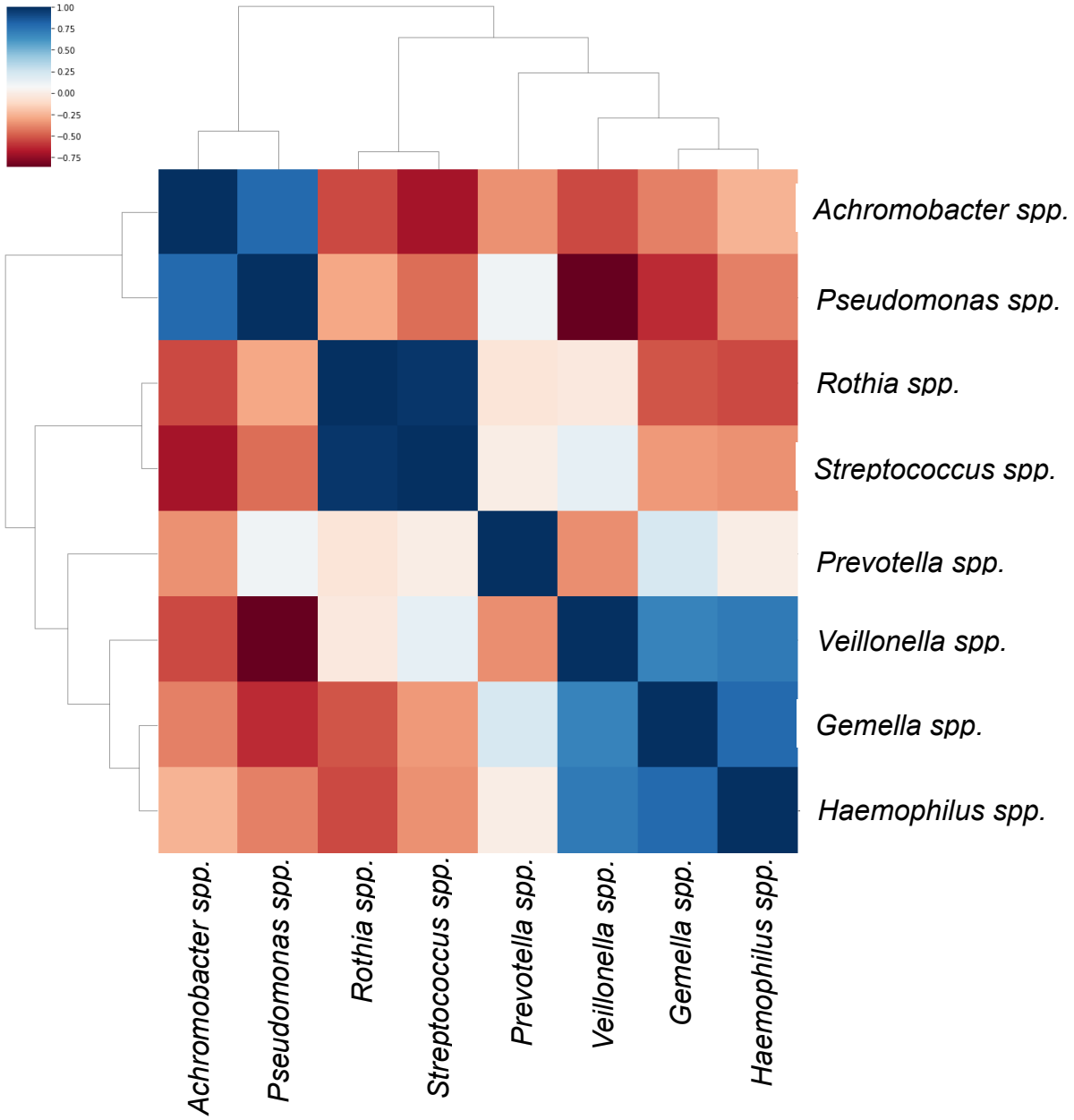

Supplementary Figure 2.1: Hierarchically clustered heatmaps of Spearman's correlation coefficients calculated using the relative abundances of a subset of five of the CF sputum metagenomes from Figure 2.2.

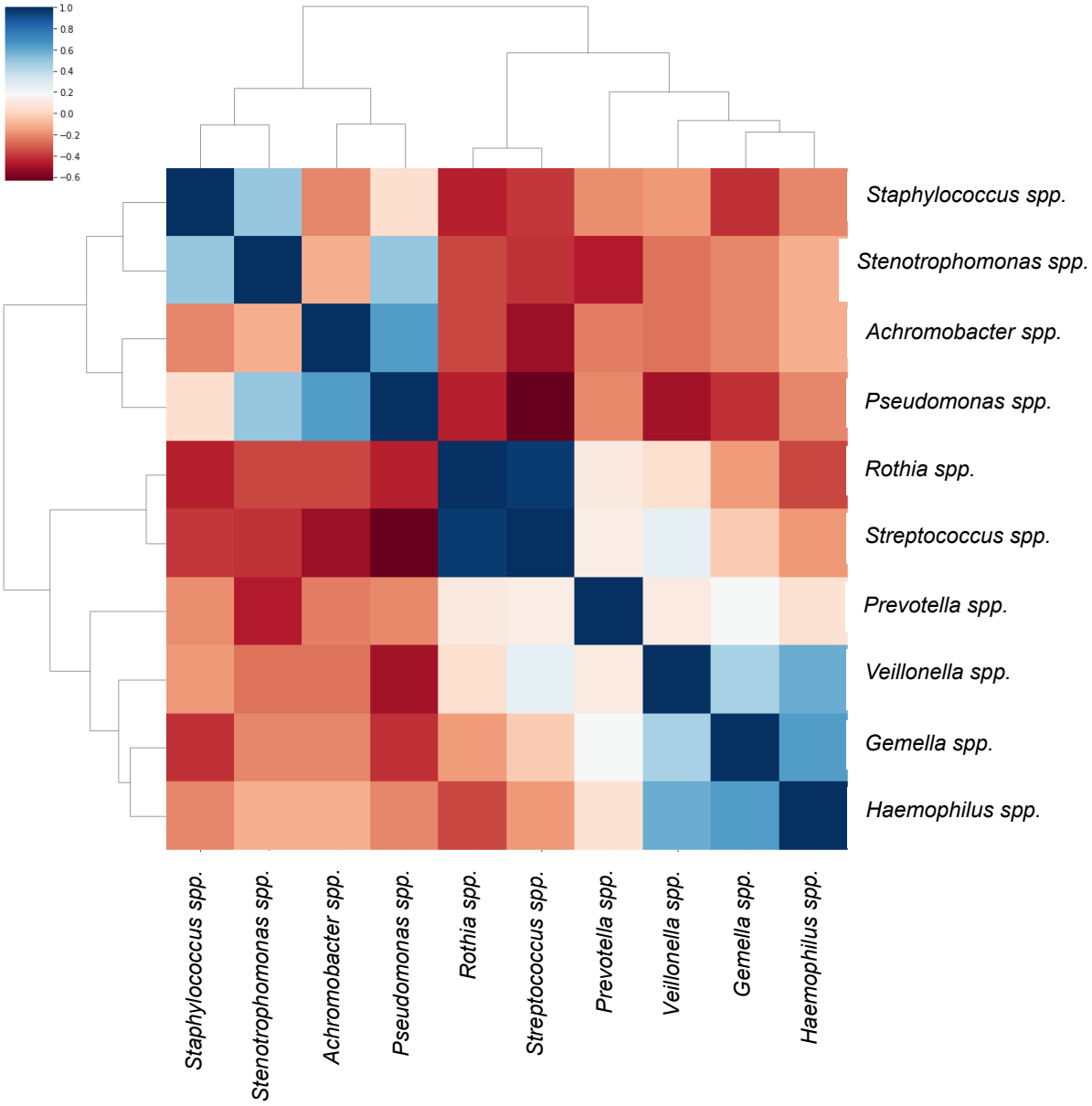

Supplementary Figure 2.2: Hierarchically clustered heatmaps of Spearman's correlation coefficients calculated using the relative abundances of subset of 10 of the CF sputum metagenomes from Figure 2.2.

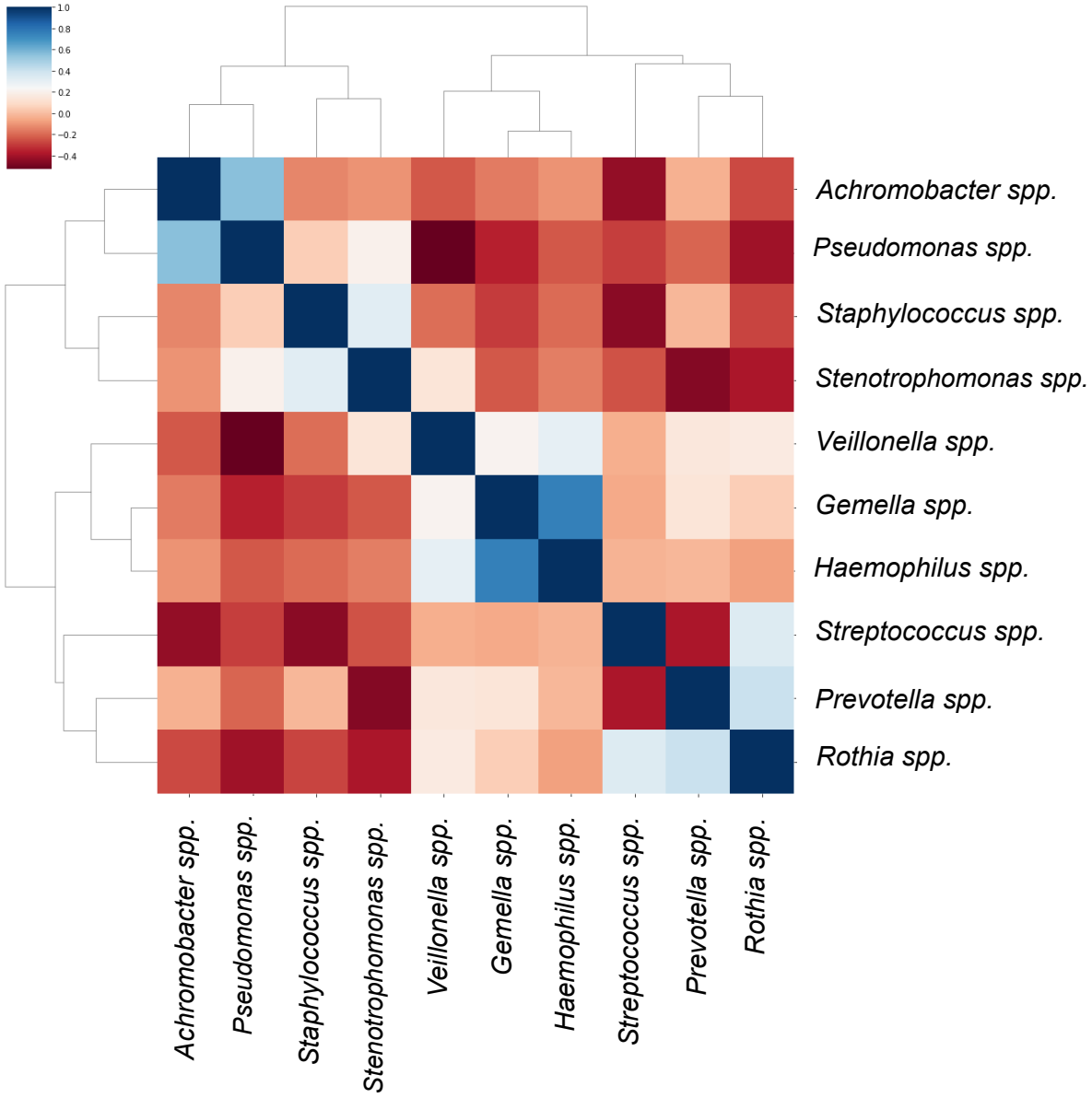

Supplementary Figure 2.3: Hierarchically clustered heatmaps of Spearman's correlation coefficients calculated using the relative abundances of subset of 15 of the CF sputum metagenomes from Figure 2.2.

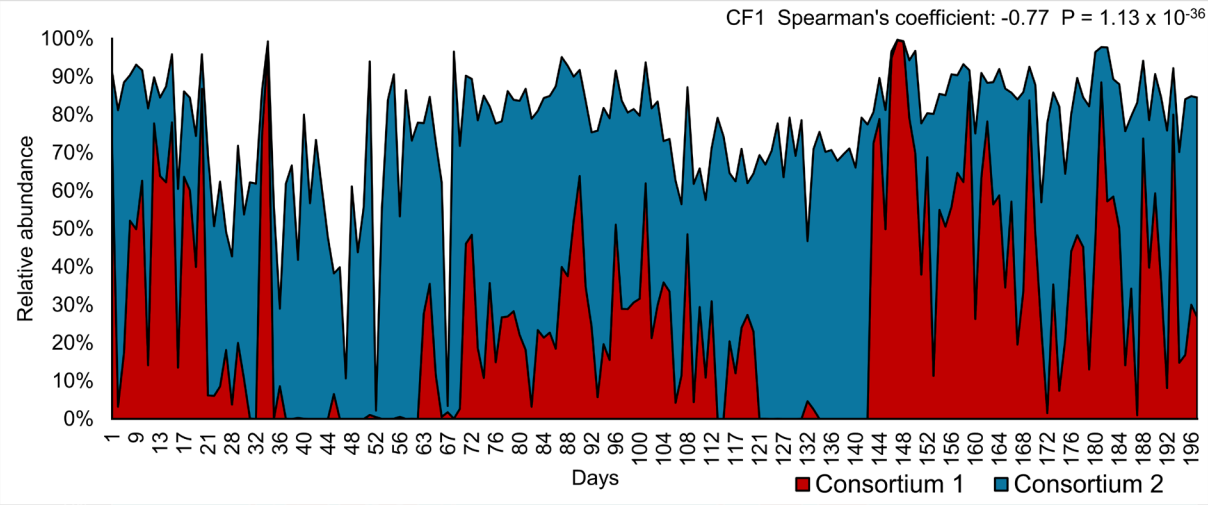

Supplementary Figure 2.4: Longitudinal dataset of sputum metagenomes from a single patient, CF1, presented as stacked area plots of the relative abundance of bacteria belonging to each consortium as a percent of the total bacteria in that sample. Bacteria not assigned to one of the two consortia defined in Figure 2.1 are represented as the white space between 100% and the edge of consortium 2. Spearman's correlation coefficient denotes the magnitude of the correlation between consortium 1 and consortium 2 over time as well as defining the relationship as either a positive or a negative correlation.

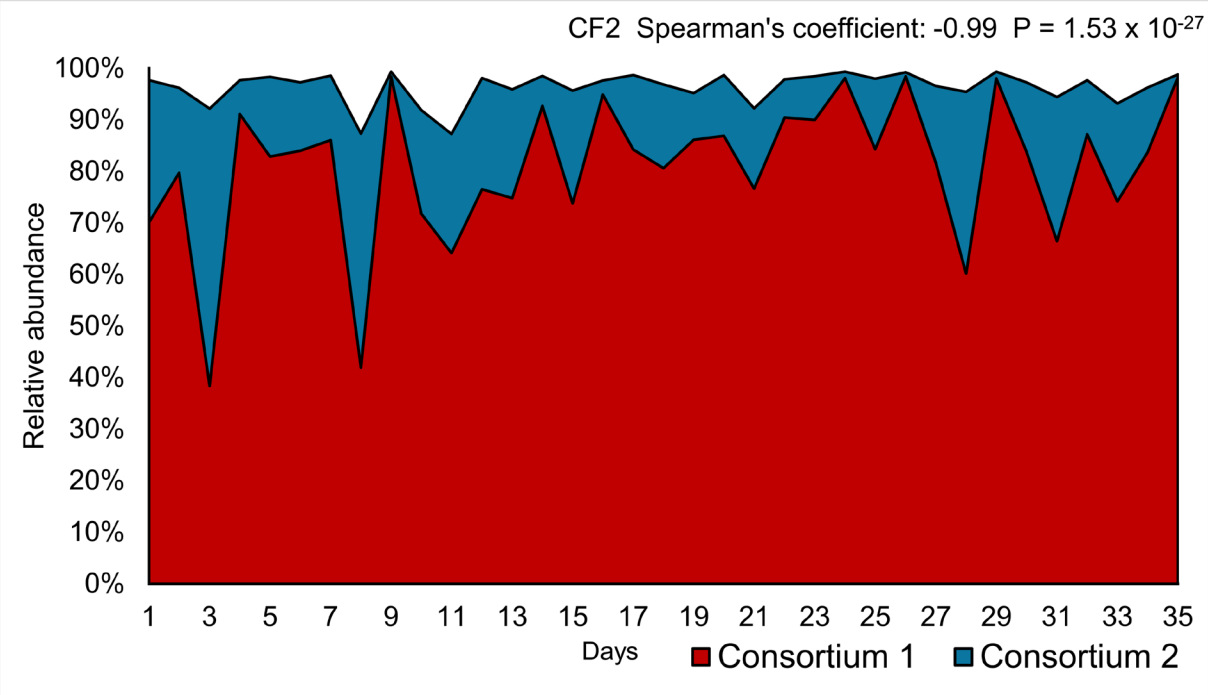

Supplementary Figure 2.5: Longitudinal dataset of sputum metagenomes from a single patient, CF2, presented as stacked area plots of the relative abundance of bacteria belonging to each consortium as a percent of the total bacteria in that sample. Bacteria not assigned to one of the two consortia defined in Figure 2.1 are represented as the white space between 100% and the edge of consortium 2. Spearman's correlation coefficient denotes the magnitude of the correlation between consortium 1 and consortium 2 over time as well as defining the relationship as either a positive or a negative correlation.

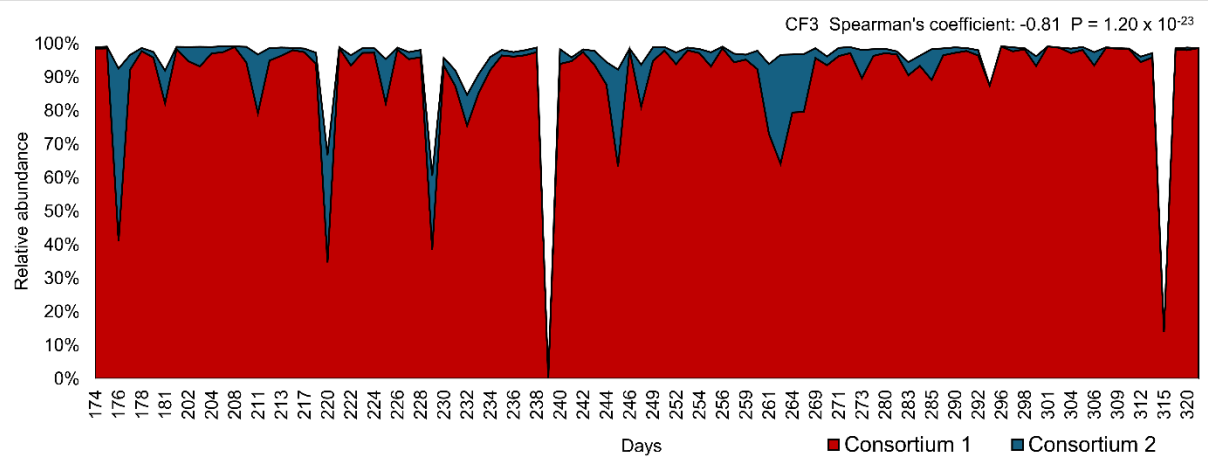

Supplementary Figure 2.6: Longitudinal dataset of sputum metagenomes from a single patient, CF3, presented as stacked area plots of the relative abundance of bacteria belonging to each consortium as a percent of the total bacteria in that sample. Bacteria not assigned to one of the two consortia defined in Figure 2.1 are represented as the white space between 100% and the edge of consortium 2. Spearman's correlation coefficient denotes the magnitude of the correlation between consortium 1 and consortium 2 over time as well as defining the relationship as either a positive or a negative correlation.

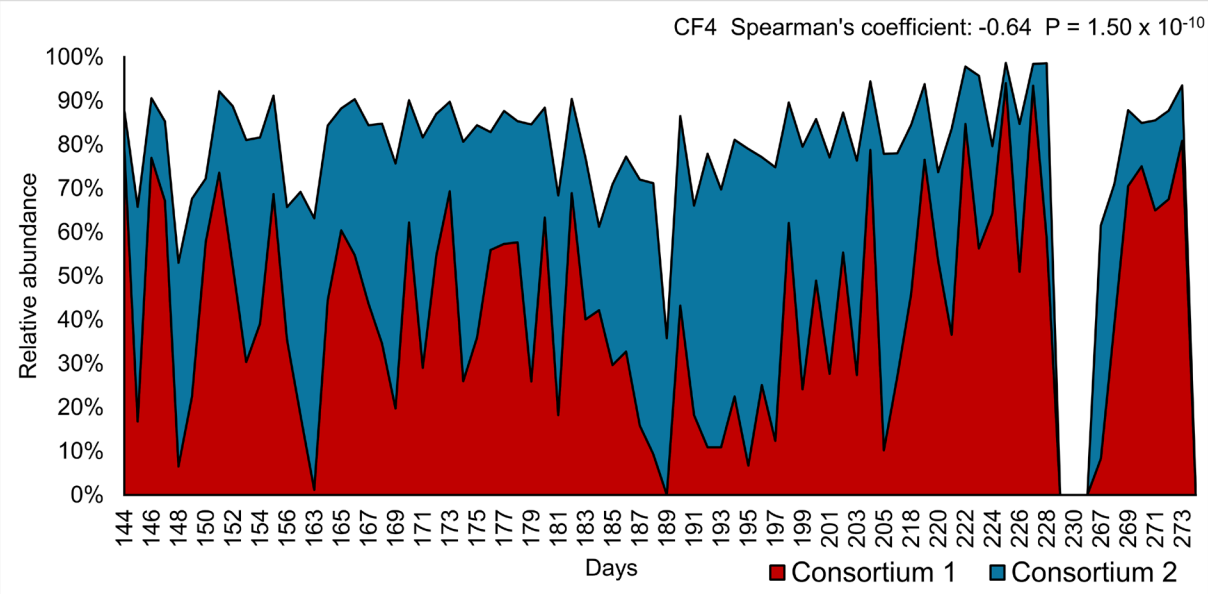

Supplementary Figure 2.7: Longitudinal dataset of sputum metagenomes from a single patient, CF4, presented as stacked area plots of the relative abundance of bacteria belonging to each consortium as a percent of the total bacteria in that sample. Bacteria not assigned to one of the two consortia defined in Figure 2.1 are represented as the white space between 100% and the edge of consortium 2. Spearman's correlation coefficient denotes the magnitude of the correlation between consortium 1 and consortium 2 over time as well as defining the relationship as either a positive or a negative correlation.

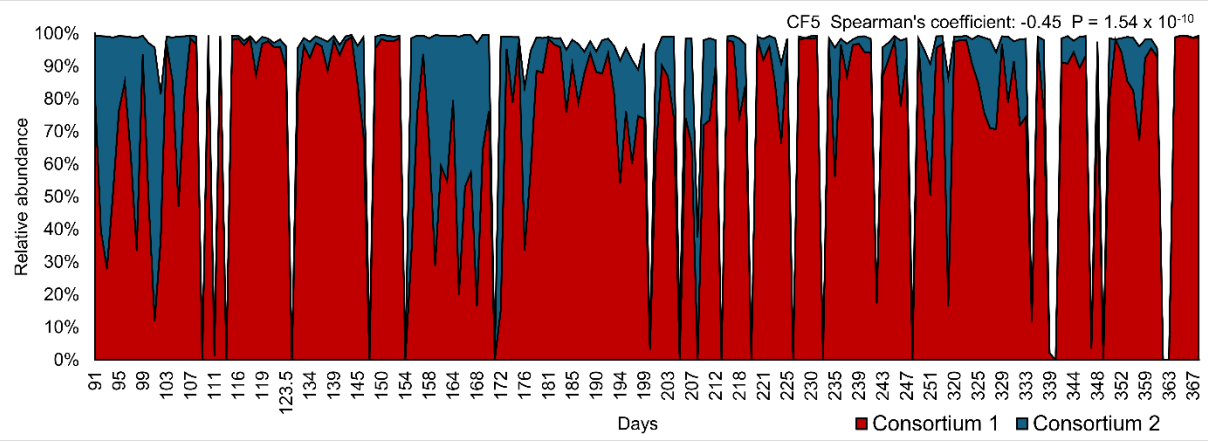

Supplementary Figure 2.8: Longitudinal dataset of sputum metagenomes from a single patient, CF5, presented as stacked area plots of the relative abundance of bacteria belonging to each consortium as a percent of the total bacteria in that sample. Bacteria not assigned to one of the two consortia defined in Figure 2.1 are represented as the white space between 100% and the edge of consortium 2. Spearman's correlation coefficient denotes the magnitude of the correlation between consortium 1 and consortium 2 over time as well as defining the relationship as either a positive or a negative correlation.

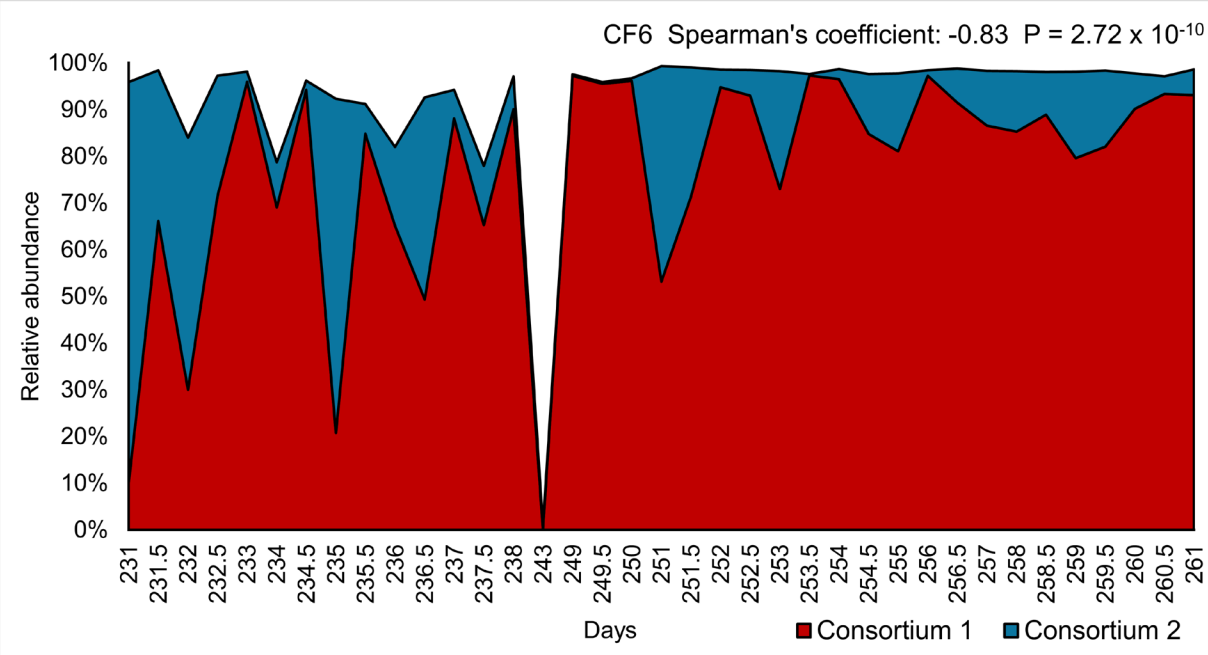

Supplementary Figure 2.9: Longitudinal dataset of sputum metagenomes from a single patient, CF6, presented as stacked area plots of the relative abundance of bacteria belonging to each consortium as a percent of the total bacteria in that sample. Bacteria not assigned to one of the two consortia defined in Figure 2.1 are represented as the white space between 100% and the edge of consortium 2. Spearman's correlation coefficient denotes the magnitude of the correlation between consortium 1 and consortium 2 over time as well as defining the relationship as either a positive or a negative correlation.

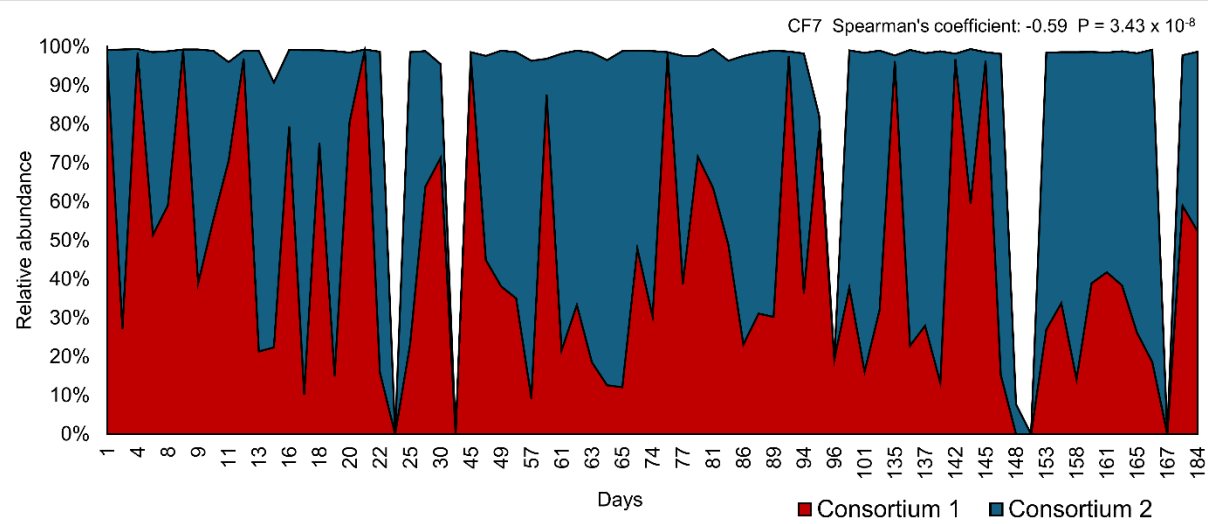

Supplementary Figure 2.10: Longitudinal dataset of sputum metagenomes from a single patient, CF7, presented as stacked area plots of the relative abundance of bacteria belonging to each consortium as a percent of the total bacteria in that sample. Bacteria not assigned to one of the two consortia defined in Figure 2.1 are represented as the white space between 100% and the edge of consortium 2. Spearman's correlation coefficient denotes the magnitude of the correlation between consortium 1 and consortium 2 over time as well as defining the relationship as either a positive or a negative correlation.

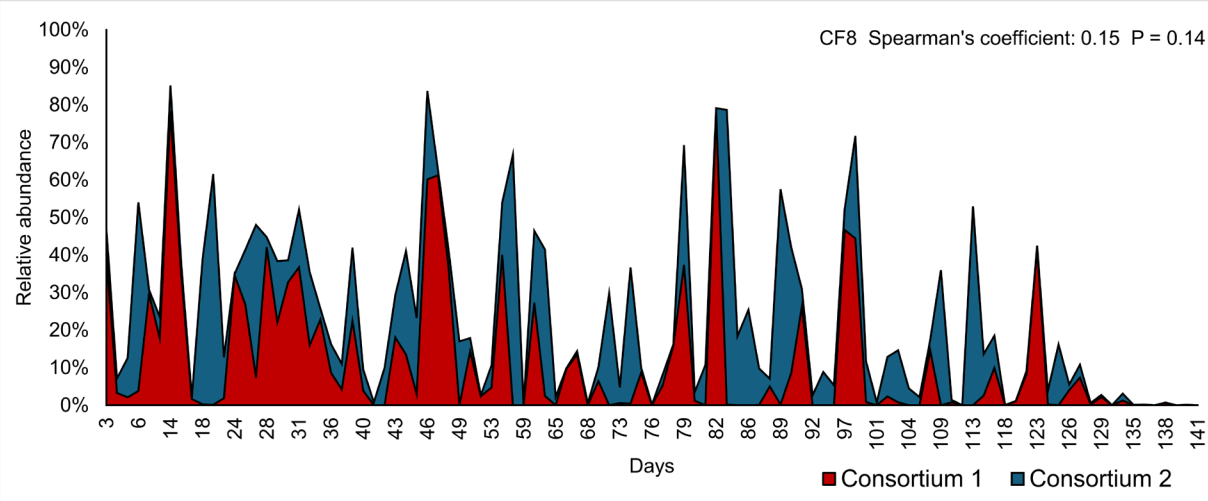

Supplementary Figure 2.11: Longitudinal dataset of sputum metagenomes from a single patient, CF8, presented as stacked area plots of the relative abundance of bacteria belonging to each consortium as a percent of the total bacteria in that sample. Bacteria not assigned to one of the two consortia defined in Figure 2.1 are represented as the white space between 100% and the edge of consortium 2. Spearman's correlation coefficient denotes the magnitude of the correlation between consortium 1 and consortium 2 over time as well as defining the relationship as either a positive or a negative correlation.

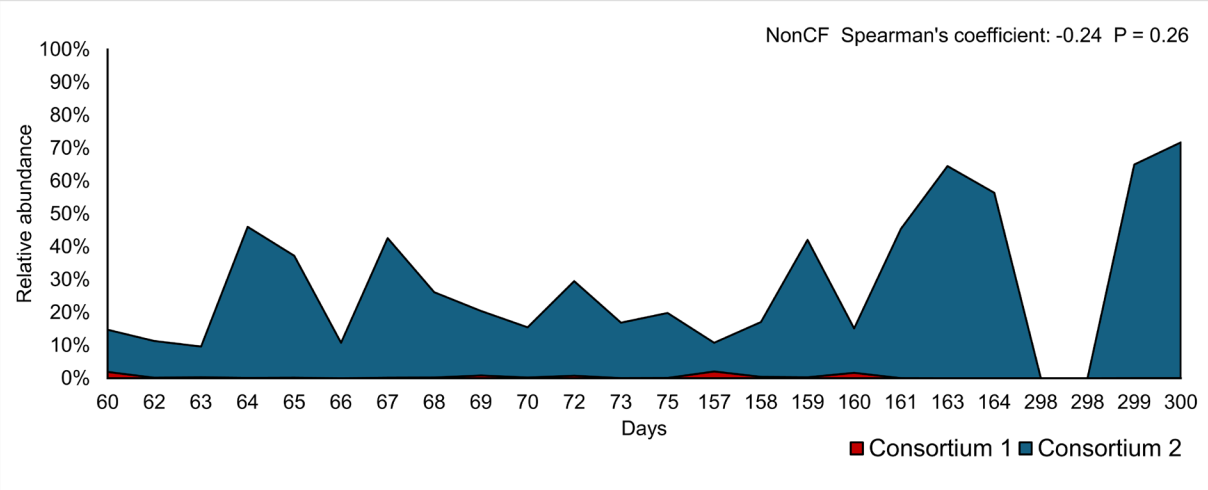

Supplementary Figure 2.12: Longitudinal dataset of sputum metagenomes from a single patient, NonCF, presented as stacked area plots of the relative abundance of bacteria belonging to each consortium as a percent of the total bacteria in that sample. Bacteria not assigned to one of the two consortia defined in Figure 2.1 are represented as the white space between 100% and the edge of consortium 2. Spearman's correlation coefficient denotes the magnitude of the correlation between consortium 1 and consortium 2 over time as well as defining the relationship as either a positive or a negative correlation.

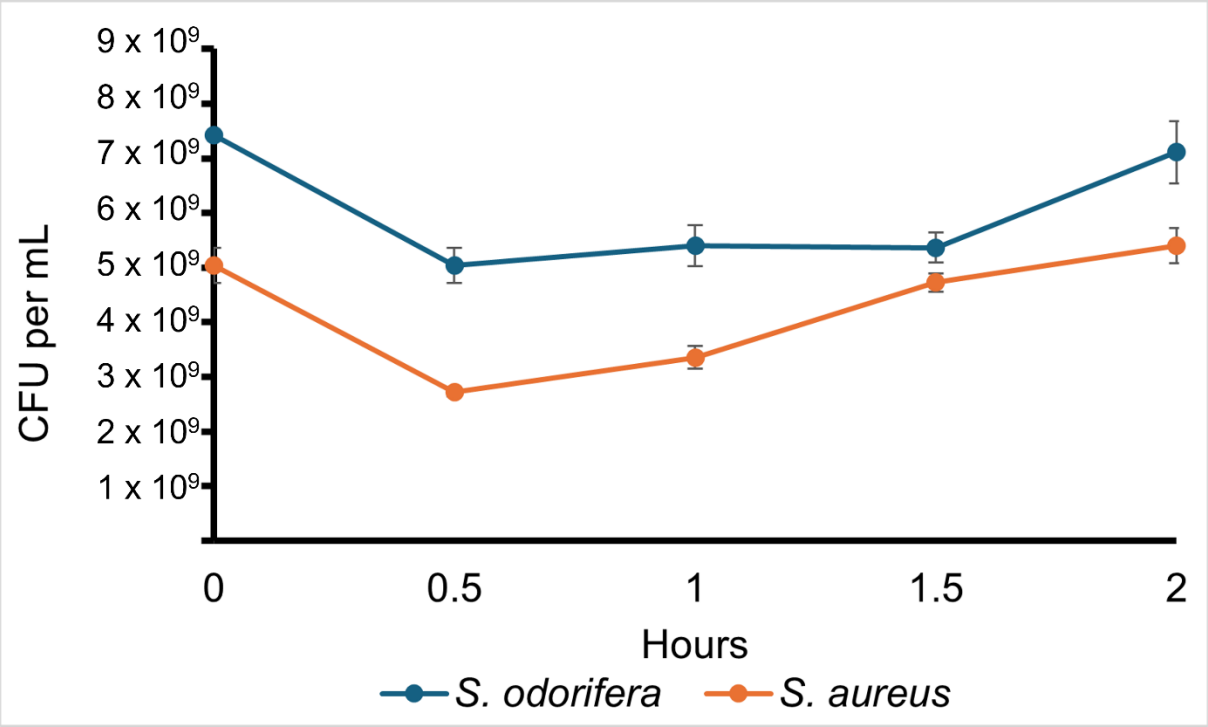

Supplementary Figure 3.1: Time series of bacterial abundances taken of stationary phase cells suspended in nutrient free SM buffer before and after treatment with tailocin John Henry. Error bars are the standard deviation of three replicates.

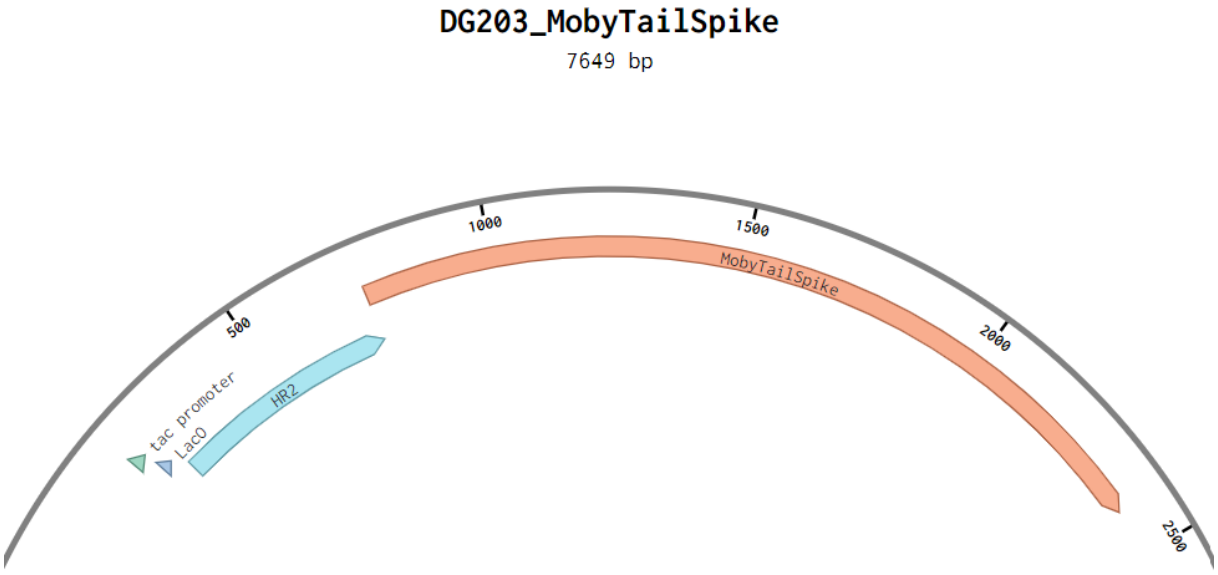

Supplementary Figure 3.2: Vector map of the shuttle vector used to make MobyWanKenobi.

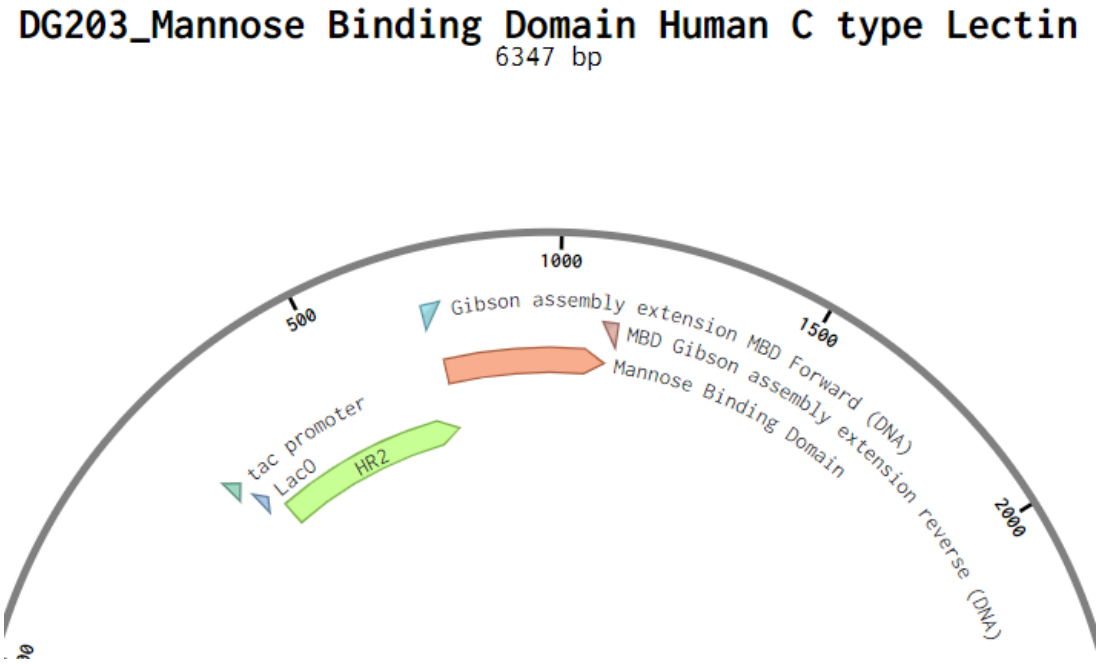

Supplementary Figure 3.3: Vector map of the shuttle vector used to make John Henry.

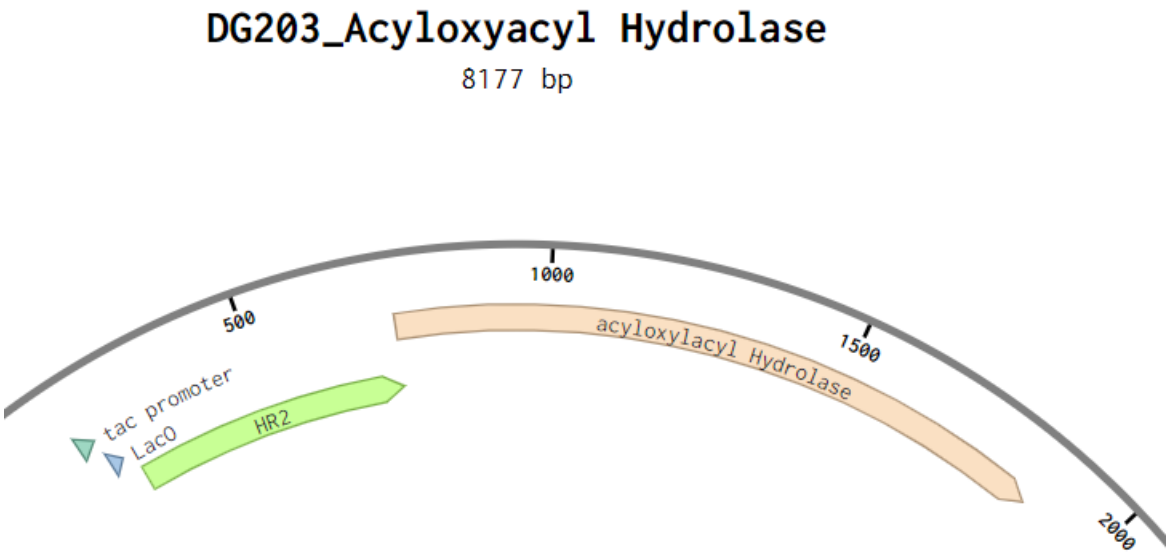

Supplementary Figure 3.4: Vector map with R2's truncated tailfiber fused to acyloxyacyl hydrolase.

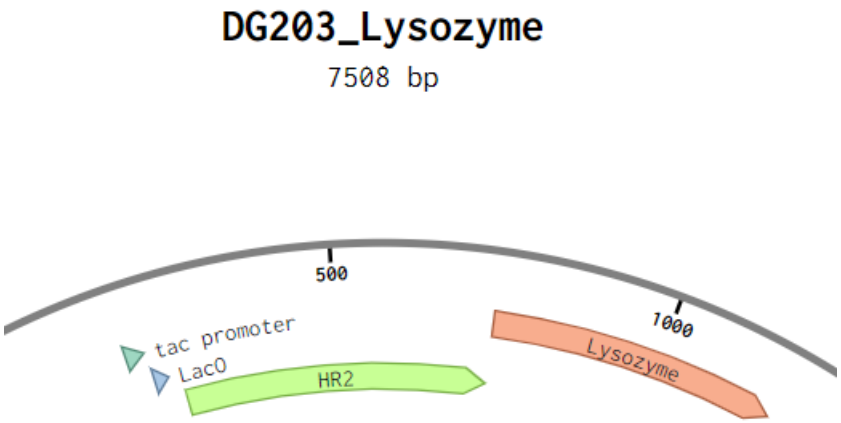

Supplementary Figure 3.5: Vector map with R2's truncated tailfiber fused to lysozyme.

Supplementary Table 3.1: Primer sequences used to make constructs used in chapter 3.

John Henry Gibson Forward	gactgggtgaaggaaaagctttttaaaggcaatttttactattttag
John Henry Gibson Reverse	gcctgcaggtcgactctagattatttgcaaatgaacagaaag
MobyWanKenobi Gibson Forward	gactgggtgaaggaaaagcttatgactgatcagattcatggc
MobyWanKenobi Gibson Reverse	catgcctgcaggtcgactctagattaattgagccagatttgag
Acyloxyacyl hydrolase Gibson Forward	gactgggtgaaggaaaagcttatgcagagcccgtggaaaattct
Acyloxyacyl hydrolase Gibson Reverse	gttcttctcctttactcatttacatcgcgtaaatcacaatg
Lysozyme Gibson Forward	gactgggtgaaggaaaagcttatgcgtagcctgctgattc
Lysozym Gibson Reverse	gttcttctcctttactcatttacaggcggcagccacgaatc

Supplementary Table 3.2: Strains used for tailocin production.

Tailocin	Plasmid	Segall lab strain designation	*G. species*
John Henry	DG203_MBD (mannose binding domain)	B45	*P. aeruginosa*
MobyWanKenobi	DG203_MobyTailSpike	B49	*P. aeruginosa*
Acyloxyacyl hydrolase	DG203_Acyloxyacyl hydrolase (A.Hase)	B43	*P. aeruginosa*
Lysozyme	DG203_lysozyme (Zyme)	B44	*P. aeruginosa*

REFERENCES

Abraham, E. P. (1939). Some properties of egg-white lysozyme. *Biochemical Journal*, *33*(4), 622–630. https://www.ncbi.nlm.nih.gov/pmc/articles/PMC1264419/

Arkin, A. P., Cottingham, R. W., Henry, C. S., Harris, N. L., Stevens, R. L., Maslov, S., Dehal, P., Ware, D., Perez, F., Canon, S., Sneddon, M. W., Henderson, M. L., Riehl, W. J., Murphy-Olson, D., Chan, S. Y., Kamimura, R. T., Kumari, S., Drake, M. M., Brettin, T. S., … Yu, D. (2018). KBase: The United States Department of Energy Systems Biology Knowledgebase. *Nature Biotechnology*, *36*(7), 566–569. https://doi.org/10.1038/nbt.4163

Bahamondez-Canas, T., & Smyth, H. D. C. (2018). Influence of Excipients on the Antimicrobial Activity of Tobramycin Against *Pseudomonas aeruginosa* Biofilms. *Pharmaceutical Research*, *35*(1), 10. https://doi.org/10.1007/s11095-017-2301-5

Bar-On, Y. M., Flamholz, A., Phillips, R., & Milo, R. (2020). SARS-CoV-2 (COVID-19) by the numbers. *eLife*, *9*, e57309. https://doi.org/10.7554/eLife.57309

Bensel, T., Stotz, M., Borneff-Lipp, M., Wollschläger, B., Wienke, A., Taccetti, G., Campana, S., Meyer, K. C., Jensen, P. Ø., Lechner, U., Ulrich, M., Döring, G., & Worlitzsch, D. (2011). Lactate in cystic fibrosis sputum. *Journal of Cystic Fibrosis: Official Journal of the European Cystic Fibrosis Society*, *10*(1), 37–44. https://doi.org/10.1016/j.jcf.2010.09.004

Boucher, R. C. (2004). New concepts of the pathogenesis of cystic fibrosis lung disease. *European Respiratory Journal*, *23*(1), 146–158. https://doi.org/10.1183/09031936.03.00057003

Bradley, J. S., Hajama, H., Akong, K., Jordan, M., Stout, D., Rowe, R. S., Conrad, D. J., Hingtgen, S., & Segall, A. M. (2023). Bacteriophage Therapy of Multidrug-resistant *Achromobacter* in an 11-Year-old Boy With Cystic Fibrosis Assessed

by Metagenome Analysis. *The Pediatric Infectious Disease Journal*, *42*(9), 754–759. https://doi.org/10.1097/INF.0000000000004000

Castner, L. M., Zimbric, M., Cahalan, S., Powell, C., & Caverly, L. J. (2021). Outcomes of cystic fibrosis pulmonary exacerbations treated with antibiotics with activity against anaerobic bacteria. *Journal of Cystic Fibrosis*, *20*(6), 926–931. https://doi.org/10.1016/j.jcf.2021.02.001

Chen, A. I., Dolben, E. F., Okegbe, C., Harty, C. E., Golub, Y., Thao, S., Ha, D. G., Willger, S. D., O'Toole, G. A., Harwood, C. S., Dietrich, L. E. P., & Hogan, D. A. (2014). *Candida albicans* Ethanol Stimulates *Pseudomonas aeruginosa* WspR-Controlled Biofilm Formation as Part of a Cyclic Relationship Involving Phenazines. *PLoS Pathogens*, *10*(10), e1004480. https://doi.org/10.1371/journal.ppat.1004480

Chen, K., & Pachter, L. (2005). Bioinformatics for Whole-Genome Shotgun Sequencing of Microbial Communities. *PLoS Computational Biology*, *1*(2), e24. https://doi.org/10.1371/journal.pcbi.0010024

Chung, C. T., Niemela, S. L., & Miller, R. H. (1989). One-step preparation of competent Escherichia coli: Transformation and storage of bacterial cells in the same solution. *Proceedings of the National Academy of Sciences of the United States of America*, *86*(7), 2172–2175. https://www.ncbi.nlm.nih.gov/pmc/articles/PMC286873/

Ciotti, M., Angeletti, S., Minieri, M., Giovannetti, M., Benvenuto, D., Pascarella, S., Sagnelli, C., Bianchi, M., Bernardini, S., & Ciccozzi, M. (2019). COVID-19 Outbreak: An Overview. *Chemotherapy*, *64*(5–6), 215–223. https://doi.org/10.1159/000507423

Cobián Güemes, A. G., Lim, Y. W., Quinn, R. A., Conrad, D. J., Benler, S., Maughan, H., Edwards, R., Brettin, T., Cantú, V. A., Cuevas, D., Hamidi, R., Dorrestein, P., & Rohwer, F. (2019a). Cystic Fibrosis Rapid Response: Translating Multi-omics Data into Clinically Relevant Information. *mBio*, *10*(2), e00431-19. https://doi.org/10.1128/mBio.00431-19

Cobián Güemes, A. G., Lim, Y. W., Quinn, R. A., Conrad, D. J., Benler, S., Maughan, H., Edwards, R., Brettin, T., Cantú, V. A., Cuevas, D., Hamidi, R., Dorrestein, P., & Rohwer, F. (2019b). Cystic Fibrosis Rapid Response: Translating Multi-omics Data into Clinically Relevant Information. *mBio*, *10*(2), e00431-19. https://doi.org/10.1128/mBio.00431-19

Colina, A. R., Aumont, F., Deslauriers, N., Belhumeur, P., & de Repentigny, L. (1996). Evidence for degradation of gastrointestinal mucin by *Candida albicans* secretory aspartyl proteinase. *Infection and Immunity*, *64*(11), 4514–4519. https://doi.org/10.1128/iai.64.11.4514-4519.1996

Conrad, D., Haynes, M., Salamon, P., Rainey, P. B., Youle, M., & Rohwer, F. (2013a). Cystic fibrosis therapy: A community ecology perspective. *American Journal of Respiratory Cell and Molecular Biology*, *48*(2), 150–156. https://doi.org/10.1165/rcmb.2012-0059PS

Conrad, D., Haynes, M., Salamon, P., Rainey, P. B., Youle, M., & Rohwer, F. (2013b). Cystic Fibrosis Therapy: A Community Ecology Perspective. *American Journal of Respiratory Cell and Molecular Biology*, *48*(2), 150–156. https://doi.org/10.1165/rcmb.2012-0059PS

Conrad, D. J., & Bailey, B. A. (2015). Multidimensional Clinical Phenotyping of an Adult Cystic Fibrosis Patient Population. *PLOS ONE*, *10*(3), e0122705. https://doi.org/10.1371/journal.pone.0122705

Conrad, D. J., Bailey, B. A., Hardie, J. A., Bakke, P. S., Eagan, T. M. L., & Aarli, B. B. (2017). Median regression spline modeling of longitudinal FEV1 measurements in cystic fibrosis (CF) and chronic obstructive pulmonary disease (COPD) patients. *PLOS ONE*, *12*(12), e0190061. https://doi.org/10.1371/journal.pone.0190061

Cornforth, D. M., Diggle, F. L., Melvin, J. A., Bomberger, J. M., & Whiteley, M. (2020). Quantitative Framework for Model Evaluation in Microbiology Research Using *Pseudomonas aeruginosa* and Cystic Fibrosis Infection as a Test Case. *mBio*, *11*(1), e03042-19. https://doi.org/10.1128/mBio.03042-19

Crouch, L. I., Liberato, M. V., Urbanowicz, P. A., Baslé, A., Lamb, C. A., Stewart, C. J., Cooke, K., Doona, M., Needham, S., Brady, R. R., Berrington, J. E., Madunic, K., Wuhrer, M., Chater, P., Pearson, J. P., Glowacki, R., Martens, E. C., Zhang, F., Linhardt, R. J., … Bolam, D. N. (2020). Prominent members of the human gut microbiota express endo-acting O-glycanases to initiate mucin breakdown. *Nature Communications*, *11*(1), Article 1. https://doi.org/10.1038/s41467-020-17847-5

Cuthbertson, L., Walker, A. W., Oliver, A. E., Rogers, G. B., Rivett, D. W., Hampton, T. H., Ashare, A., Elborn, J. S., De Soyza, A., Carroll, M. P., Hoffman, L. R., Lanyon, C., Moskowitz, S. M., O'Toole, G. A., Parkhill, J., Planet, P. J., Teneback, C. C., Tunney, M. M., Zuckerman, J. B., … Van Der Gast, C. J. (2020). Lung function and microbiota diversity in cystic fibrosis. *Microbiome*, *8*(1), 45. https://doi.org/10.1186/s40168-020-00810-3

Cystic Fibrosis Foundation. (2021). *2021 Annual Data Report*.

Da Silva Sanchez, A., Paunovska, K., Cristian, A., & Dahlman, J. E. (2020). Treating Cystic Fibrosis with mRNA and CRISPR. *Human Gene Therapy*, *31*(17–18), 940–955. https://doi.org/10.1089/hum.2020.137

Damé-Teixeira, N., Parolo, C. C. F., Maltz, M., Rup, A. G., Devine, D. A., & Do, T. (2018). Gene expression of bacterial collagenolytic proteases in root caries. *Journal of Oral Microbiology*, *10*(1), 1424475. https://doi.org/10.1080/20002297.2018.1424475

del Rio, B., Redruello, B., Linares, D. M., Ladero, V., Ruas-Madiedo, P., Fernandez, M., Martin, M. C., & Alvarez, M. A. (2019). The biogenic amines putrescine and cadaverine show in vitro cytotoxicity at concentrations that can be found in foods. *Scientific Reports*, *9*(1), Article 1. https://doi.org/10.1038/s41598-018-36239-w

Dickinson, C. J., Reed, M. D., Stern, R. C., Aronoff, S. C., Yamashita, T. S., & Blumer, J. L. (1988). The effect of exocrine pancreatic function on chloramphenicol pharmacokinetics in patients with cystic fibrosis. *Pediatric Research*, *23*(4), 388–392. https://doi.org/10.1203/00006450-198804000-00009

Fajac, I., & Sermet-Gaudelus, I. (2021). Therapeutic pipeline for individuals with cystic fibrosis with mutations nonresponsive to current cystic fibrosis transmembrane conductance regulator modulators. *Current Opinion in Pulmonary Medicine*, *27*(6), 567. https://doi.org/10.1097/MCP.0000000000000827

Flynn, J. M., Niccum, D., Dunitz, J. M., & Hunter, R. C. (2016). Evidence and Role for Bacterial Mucin Degradation in Cystic Fibrosis Airway Disease. *PLOS Pathogens*, *12*(8), e1005846. https://doi.org/10.1371/journal.ppat.1005846

Garg, N., Wang, M., Hyde, E., Da Silva, R. R., Melnik, A. V., Protsyuk, I., Bouslimani, A., Lim, Y. W., Wong, R., Humphrey, G., Ackermann, G., Spivey, T., Brouha, S. S., Bandeira, N., Lin, G. Y., Rohwer, F., Conrad, D. J., Alexandrov, T., Knight, R., & Dorrestein, P. C. (2017). Three-Dimensional Microbiome and Metabolome Cartography of a Diseased Human Lung. *Cell Host & Microbe*, *22*(5), 705-716.e4. https://doi.org/10.1016/j.chom.2017.10.001

Gebreyohannes, G., Nyerere, A., Bii, C., & Sbhatu, D. B. (2019). Challenges of intervention, treatment, and antibiotic resistance of biofilm-forming microorganisms. *Heliyon*, *5*(8), e02192. https://doi.org/10.1016/j.heliyon.2019.e02192

Ghequire, M. G. K., & De Mot, R. (2015). The Tailocin Tale: Peeling off Phage Tails. *Trends in Microbiology*, *23*(10), 587–590. https://doi.org/10.1016/j.tim.2015.07.011

González-Pastor, J. E., Hobbs, E. C., & Losick, R. (2003). Cannibalism by sporulating bacteria. *Science (New York, N.Y.)*, *301*(5632), 510–513. https://doi.org/10.1126/science.1086462

Grasemann, H., Shehnaz, D., Enomoto, M., Leadley, M., Belik, J., & Ratjen, F. (2012). L-ornithine derived polyamines in cystic fibrosis airways. *PloS One*, *7*(10), e46618. https://doi.org/10.1371/journal.pone.0046618

Hewitt, L. F. (1931). Effect of lysozyme on the oxidation-reduction potentials of *M. lysodeikticus* cultures. *Biochemical Journal*, *25*(5), 1452–1457. https://www.ncbi.nlm.nih.gov/pmc/articles/PMC1260771/

Jiang, H., White, E. J., Ríos-Vicil, C. I., Xu, J., Gomez-Manzano, C., & Fueyo, J. (2011). Human Adenovirus Type 5 Induces Cell Lysis through Autophagy and Autophagy-Triggered Caspase Activity ▿ . *Journal of Virology*, *85*(10), 4720–4729. https://doi.org/10.1128/JVI.02032-10

Kandel, P. P., Baltrus, D. A., & Hockett, K. L. (2020). Pseudomonas Can Survive Tailocin Killing via Persistence-Like and Heterogenous Resistance Mechanisms. *Journal of Bacteriology*, *202*(13), e00142-20. https://doi.org/10.1128/JB.00142-20

Kinsella, R. A., & Swift, H. F. (1918). THE CLASSIFICATION OF HEMOLYTIC STREPTOCOCCI. *The Journal of Experimental Medicine*, *28*(2), 169–180. https://doi.org/10.1084/jem.28.2.169

Lim, Y. W., Evangelista, J. S., Schmieder, R., Bailey, B., Haynes, M., Furlan, M., Maughan, H., Edwards, R., Rohwer, F., & Conrad, D. (2014). Clinical Insights from Metagenomic Analysis of Sputum Samples from Patients with Cystic Fibrosis. *Journal of Clinical Microbiology*, *52*(2), 425–437. https://doi.org/10.1128/JCM.02204-13

Lim, Y. W., Schmieder, R., Haynes, M., Furlan, M., Matthews, T. D., Whiteson, K., Poole, S. J., Hayes, C. S., Low, D. A., Maughan, H., Edwards, R., Conrad, D., & Rohwer, F. (2013). Mechanistic Model of *Rothia mucilaginosa* Adaptation toward Persistence in the CF Lung, Based on a Genome Reconstructed from Metagenomic Data. *PLoS ONE*, *8*(5), e64285. https://doi.org/10.1371/journal.pone.0064285

Lim, Y. W., Schmieder, R., Haynes, M., Willner, D., Furlan, M., Youle, M., Abbott, K., Edwards, R., Evangelista, J., Conrad, D., & Rohwer, F. (2013). Metagenomics and metatranscriptomics: Windows on CF-associated viral and microbial communities. *Journal of Cystic Fibrosis*, *12*(2), 154–164. https://doi.org/10.1016/j.jcf.2012.07.009

Lu, J., Carmody, L. A., Opron, K., Simon, R. H., Kalikin, L. M., Caverly, L. J., & LiPuma, J. J. (2020). Parallel Analysis of Cystic Fibrosis Sputum and Saliva Reveals Overlapping Communities and an Opportunity for Sample Decontamination. *mSystems*, *5*(4), e00296-20. https://doi.org/10.1128/mSystems.00296-20

Luo, Y., & Song, Y. (2021). Mechanism of Antimicrobial Peptides: Antimicrobial, Anti-Inflammatory and Antibiofilm Activities. *International Journal of Molecular Sciences*, *22*(21), 11401. https://doi.org/10.3390/ijms222111401

Marchandin, H., Teyssier, C., Campos, J., Jean-Pierre, H., Roger, F., Gay, B., Carlier, J.-P., & Jumas-Bilak, E. (2010). Negativicoccus succinicivorans gen. Nov., sp. Nov., isolated from human clinical samples, emended description of the family Veillonellaceae and description of Negativicutes classis nov., Selenomonadales ord. Nov. And Acidaminococcaceae fam. Nov. In the bacterial phylum Firmicutes. *International Journal of Systematic and Evolutionary Microbiology*, *60*(Pt 6), 1271–1279. https://doi.org/10.1099/ijs.0.013102-0

Martin, C., Guzior, D. V., Gonzalez, C. T., Okros, M., Mielke, J., Padillo, L., Querido, G., Gil, M., Thomas, R., McClelland, M., Conrad, D., Widder, S., & Quinn, R. A. (2023). Longitudinal Microbial and Molecular Dynamics in the Cystic Fibrosis Lung after Elexacaftor-Tezacaftor-Ivacaftor therapy. *Research Square*, rs.3.rs-3356170. https://doi.org/10.21203/rs.3.rs-3356170/v1

Martin, D. W. Jr., Jamieson, A. C., Scholl, D. M., & Williams, S. R. (2010). *Modified bacteriocins and methods for their use* (United States Patent US7732586B2). https://patents.google.com/patent/US7732586B2/en?inventor=Dean+scholl&oq=+Dean+scholl

May, T. B., Shinabarger, D., Maharaj, R., Kato, J., Chu, L., DeVault, J. D., Roychoudhury, S., Zielinski, N. A., Berry, A., & Rothmel, R. K. (1991). Alginate synthesis by *Pseudomonas aeruginosa*: A key pathogenic factor in chronic pulmonary infections of cystic fibrosis patients. *Clinical Microbiology Reviews*, *4*(2), 191–206. https://doi.org/10.1128/CMR.4.2.191

McCarron, A., Parsons, D., & Donnelley, M. (2021). Animal and Cell Culture Models for Cystic Fibrosis: Which Model Is Right for Your Application? *The American Journal of Pathology*, *191*(2), 228–242. https://doi.org/10.1016/j.ajpath.2020.10.017

Melnik, A. V., Vázquez-Baeza, Y., Aksenov, A. A., Hyde, E., McAvoy, A. C., Wang, M., Da Silva, R. R., Protsyuk, I., Wu, J. V., Bouslimani, A., Lim, Y. W., Luzzatto-Knaan, T., Comstock, W., Quinn, R. A., Wong, R., Humphrey, G., Ackermann, G., Spivey, T., Brouha, S. S., … Garg, N. (2019). Molecular and Microbial Microenvironments in Chronically Diseased Lungs Associated with Cystic Fibrosis. *mSystems*, *4*(5), e00375-19. https://doi.org/10.1128/mSystems.00375-19

Midani, F. S., Collins, J., & Britton, R. A. (2021). AMiGA: Software for Automated Analysis of Microbial Growth Assays. *mSystems*, *6*(4), 10.1128/msystems.00508-21. https://doi.org/10.1128/msystems.00508-21

Moyne, O., Al-Bassam, M., Lieng, C., Thiruppathy, D., Norton, G. J., Kumar, M., Haddad, E., Zaramela, L. S., & Zengler, K. (2023). *Guild and Niche Determination Enable Targeted Alteration of the Microbiome* (p. 2023.05.11.540389). bioRxiv. https://doi.org/10.1101/2023.05.11.540389

mRNA Therapy for Cystic Fibrosis | Cystic Fibrosis Foundation. (n.d.). Retrieved May 15, 2024, from https://www.cff.org/research-clinical-trials/mrna-therapy-cystic-fibrosis

Nguyen, M., Sharma, A., Wu, W., Gomi, R., Sung, B., Hospodsky, D., Angenent, L. T., & Worgall, S. (2016). The fermentation product 2,3-butanediol alters P. aeruginosa clearance, cytokine response and the lung microbiome. *The ISME Journal*, *10*(12), 2978–2983. https://doi.org/10.1038/ismej.2016.76

Norton, J. F., & Bailey, J. H. (1931). LABORATORY: ISOLATION AND CULTIVATION OF THE WHOOPING COUGH BACILLUS, HEMOPHILUS PERTUSSIS. *American Journal of Public Health and the Nation's Health*, *21*(10), 1144–1147. https://doi.org/10.2105/ajph.21.10.1144

O'Brien, A. D., Newland, J. W., Miller, S. F., Holmes, R. K., Smith, H. W., & Formal, S. B. (1984). Shiga-like toxin-converting phages from *Escherichia coli* strains that cause hemorrhagic colitis or infantile diarrhea. *Science (New York, N.Y.)*, *226*(4675), 694–696. https://doi.org/10.1126/science.6387911

Olson, R. D., Assaf, R., Brettin, T., Conrad, N., Cucinell, C., Davis, J. J., Dempsey, D. M., Dickerman, A., Dietrich, E. M., Kenyon, R. W., Kuscuoglu, M., Lefkowitz, E. J., Lu, J., Machi, D., Macken, C., Mao, C., Niewiadomska, A., Nguyen, M., Olsen, G. J., … Stevens, R. L. (2023). Introducing the Bacterial and Viral Bioinformatics Resource Center (BV-BRC): A resource combining PATRIC, IRD and ViPR. *Nucleic Acids Research*, *51*(D1), D678–D689. https://doi.org/10.1093/nar/gkac1003

Orth, J. D., Thiele, I., & Palsson, B. Ø. (2010). What is flux balance analysis? *Nature Biotechnology*, *28*(3), 245–248. https://doi.org/10.1038/nbt.1614

O'Toole, G. A., Crabbé, A., Kümmerli, R., LiPuma, J. J., Bomberger, J. M., Davies, J. C., Limoli, D., Phelan, V. V., Bliska, J. B., DePas, W. H., Dietrich, L. E., Hampton, T. H., Hunter, R., Khursigara, C. M., Price-Whelan, A., Ashare, A., Cramer, R. A., Goldberg, J. B., Harrison, F., … Whiteson, K. (2021). Model Systems to Study the Chronic, Polymicrobial Infections in Cystic Fibrosis: Current Approaches and Exploring Future Directions. *mBio*, *12*(5), e0176321. https://doi.org/10.1128/mBio.01763-21

Panchabhai, T. S., Mukhopadhyay, S., Sehgal, S., Bandyopadhyay, D., Erzurum, S. C., & Mehta, A. C. (2016). Plugs of the Air Passages. *Chest*, *150*(5), 1141–1157. https://doi.org/10.1016/j.chest.2016.07.003

Passi, A., Tibocha-Bonilla, J. D., Kumar, M., Tec-Campos, D., Zengler, K., & Zuniga, C. (2022). Genome-Scale Metabolic Modeling Enables In-Depth Understanding of Big Data. *Metabolites*, *12*(1), Article 1. https://doi.org/10.3390/metabo12010014

Pohlman, T. H., Munford, R. S., & Harlan, J. M. (1987). Deacylated lipopolysaccharide inhibits neutrophil adherence to endothelium induced by

lipopolysaccharide in vitro. *The Journal of Experimental Medicine*, *165*(5), 1393–1402. https://doi.org/10.1084/jem.165.5.1393

Quinn, R. A., Adem, S., Mills, R. H., Comstock, W., DeRight Goldasich, L., Humphrey, G., Aksenov, A. A., Melnik, A. V., Da Silva, R., Ackermann, G., Bandeira, N., Gonzalez, D. J., Conrad, D., O'Donoghue, A. J., Knight, R., & Dorrestein, P. C. (2019). Neutrophilic proteolysis in the cystic fibrosis lung correlates with a pathogenic microbiome. *Microbiome*, *7*(1), 23. https://doi.org/10.1186/s40168-019-0636-3

Quinn, R. A., Comstock, W., Zhang, T., Morton, J. T., Da Silva, R., Tran, A., Aksenov, A., Nothias, L.-F., Wangpraseurt, D., Melnik, A. V., Ackermann, G., Conrad, D., Klapper, I., Knight, R., & Dorrestein, P. C. (2018). Niche partitioning of a pathogenic microbiome driven by chemical gradients. *Science Advances*, *4*(9), eaau1908. https://doi.org/10.1126/sciadv.aau1908

Quinn, R. A., Lim, Y. W., Mak, T. D., Whiteson, K., Furlan, M., Conrad, D., Rohwer, F., & Dorrestein, P. (2016). Metabolomics of pulmonary exacerbations reveals the personalized nature of cystic fibrosis disease. *PeerJ*, *4*, e2174. https://doi.org/10.7717/peerj.2174

Quinn, R. A., Lim, Y. W., Maughan, H., Conrad, D., Rohwer, F., & Whiteson, K. L. (2014). Biogeochemical Forces Shape the Composition and Physiology of Polymicrobial Communities in the Cystic Fibrosis Lung. *mBio*, *5*(2), e00956-13. https://doi.org/10.1128/mBio.00956-13

Quinn, R. A., Phelan, V. V., Whiteson, K. L., Garg, N., Bailey, B. A., Lim, Y. W., Conrad, D. J., Dorrestein, P. C., & Rohwer, F. L. (2016). Microbial, host and xenobiotic diversity in the cystic fibrosis sputum metabolome. *The ISME Journal*, *10*(6), 1483–1498. https://doi.org/10.1038/ismej.2015.207

Quinn, R. A., Whiteson, K., Lim, Y. W., Zhao, J., Conrad, D., LiPuma, J. J., Rohwer, F., & Widder, S. (2016). Ecological networking of cystic fibrosis lung infections. *Npj Biofilms and Microbiomes*, *2*(1), 4. https://doi.org/10.1038/s41522-016-0002-1

Quinn, R. A., Whiteson, K., Lim, Y.-W., Salamon, P., Bailey, B., Mienardi, S., Sanchez, S. E., Blake, D., Conrad, D., & Rohwer, F. (2015a). A Winogradsky-based culture system shows an association between microbial fermentation and cystic fibrosis exacerbation. *The ISME Journal*, *9*(4), 1024–1038. https://doi.org/10.1038/ismej.2014.234

Quinn, R. A., Whiteson, K., Lim, Y.-W., Salamon, P., Bailey, B., Mienardi, S., Sanchez, S. E., Blake, D., Conrad, D., & Rohwer, F. (2015b). A Winogradsky-based culture system shows an association between microbial fermentation and cystic fibrosis exacerbation. *The ISME Journal*, *9*(4), 1024–1038. https://doi.org/10.1038/ismej.2014.234

Richardson, A. R., Somerville, G. A., & Sonenshein, A. L. (2015). Regulating the Intersection of Metabolism and Pathogenesis in Gram-positive Bacteria. *Microbiology Spectrum*, *3*(3). https://doi.org/10.1128/microbiolspec.MBP-0004-2014

Ridley, F. (1928). Lysozyme: An Antibacterial Body present in Great Concentration in Tears, and its Relation to Infection of the Human Eye. *Proceedings of the Royal Society of Medicine*, *21*(9), 1495–1506.

Riordan, J. R., Rommens, J. M., Kerem, B., Alon, N., Rozmahel, R., Grzelczak, Z., Zielenski, J., Lok, S., Plavsic, N., & Chou, J. L. (1989). Identification of the cystic fibrosis gene: Cloning and characterization of complementary DNA. *Science (New York, N.Y.)*, *245*(4922), 1066–1073. https://doi.org/10.1126/science.2475911

Riquelme, S. A., Lozano, C., Moustafa, A. M., Liimatta, K., Tomlinson, K. L., Britto, C., Khanal, S., Gill, S. K., Narechania, A., Azcona-Gutiérrez, J. M., DiMango, E., Saénz, Y., Planet, P., & Prince, A. (2019). CFTR-PTEN-dependent mitochondrial metabolic dysfunction promotes *Pseudomonas aeruginosa* airway infection. *Science Translational Medicine*, *11*(499), eaav4634. https://doi.org/10.1126/scitranslmed.aav4634

Ritchie, J. M., Greenwich, J. L., Davis, B. M., Bronson, R. T., Gebhart, D., Williams, S. R., Martin, D., Scholl, D., & Waldor, M. K. (2011). An *Escherichia coli* O157-

specific engineered pyocin prevents and ameliorates infection by *E. coli* O157:H7 in an animal model of diarrheal disease. *Antimicrobial Agents and Chemotherapy*, *55*(12), 5469–5474. https://doi.org/10.1128/AAC.05031-11

Rivas-Santisteban, J., Yubero, P., Robaina-Estévez, S., González, J. M., Tamames, J., & Pedrós-Alió, C. (2023). *Quantifying microbial guilds* (p. 2023.07.23.550202). bioRxiv. https://doi.org/10.1101/2023.07.23.550202

Rogers, A. C., McDermott, F. D., Mohan, H. M., O'Connell, P. R., Winter, D. C., & Baird, A. W. (2015). The effects of polyamines on human colonic mucosal function. *European Journal of Pharmacology*, *764*, 157–163. https://doi.org/10.1016/j.ejphar.2015.07.006

Rowe, S. M., Zuckerman, J. B., Dorgan, D., Lascano, J., McCoy, K., Jain, M., Schechter, M. S., Lommatzsch, S., Indihar, V., Lechtzin, N., McBennett, K., Callison, C., Brown, C., Liou, T. G., MacDonald, K. D., Nasr, S. Z., Bodie, S., Vaughn, M., Meltzer, E. B., & Barbier, A. J. (2023). Inhaled mRNA therapy for treatment of cystic fibrosis: Interim results of a randomized, double-blind, placebo-controlled phase 1/2 clinical study. *Journal of Cystic Fibrosis: Official Journal of the European Cystic Fibrosis Society*, *22*(4), 656–664. https://doi.org/10.1016/j.jcf.2023.04.008

Sahu, S., & Lynn, W. S. (1978). Lipid composition of sputum from patients with asthma and patients with cystic fibrosis. *Inflammation*, *3*(1), 27–36. https://doi.org/10.1007/BF00917319

Scholl, D. (2017). Phage Tail-Like Bacteriocins. *Annual Review of Virology*, *4*(1), 453–467. https://doi.org/10.1146/annurev-virology-101416-041632

Scholl, D., Cooley, M., Williams, S. R., Gebhart, D., Martin, D., Bates, A., & Mandrell, R. (2009). An engineered R-type pyocin is a highly specific and sensitive bactericidal agent for the food-borne pathogen *Escherichia coli* O157:H7. *Antimicrobial Agents and Chemotherapy*, *53*(7), 3074–3080. https://doi.org/10.1128/AAC.01660-08

Scoffield, J., & Silo-Suh, L. (2016). Glycerol metabolism promotes biofilm formation by *Pseudomonas aeruginosa*. *Canadian Journal of Microbiology*, *62*(8), 704–710. https://doi.org/10.1139/cjm-2016-0119

Silva, E., Monteiro, R., Grainha, T., Alves, D., Pereira, M. O., & Sousa, A. M. (2020). Fostering Innovation in the Treatment of Chronic Polymicrobial Cystic Fibrosis-Associated Infections Exploring Aspartic Acid and Succinic Acid as Ciprofloxacin Adjuvants. *Frontiers in Cellular and Infection Microbiology*, *10*, 441. https://doi.org/10.3389/fcimb.2020.00441

Silveira, C. B., Cobián-Güemes, A. G., Uranga, C., Baker, J. L., Edlund, A., Rohwer, F., & Conrad, D. (2021). Multi-Omics Study of Keystone Species in a Cystic Fibrosis Microbiome. *International Journal of Molecular Sciences*, *22*(21), 12050. https://doi.org/10.3390/ijms222112050

Simberloff, D., & Dayan, T. (1991). The Guild Concept and the Structure of Ecological Communities. *Annual Review of Ecology and Systematics*, *22*(1), 115–143. https://doi.org/10.1146/annurev.es.22.110191.000555

Sønderholm, M., Koren, K., Wangpraseurt, D., Jensen, P. Ø., Kolpen, M., Kragh, K. N., Bjarnsholt, T., & Kühl, M. (2018). Tools for studying growth patterns and chemical dynamics of aggregated *Pseudomonas aeruginosa* exposed to different electron acceptors in an alginate bead model. *Npj Biofilms and Microbiomes*, *4*(1), 3. https://doi.org/10.1038/s41522-018-0047-4

Sriramulu, D. D., Lünsdorf, H., Lam, J. S., & Römling, U. (2005). Microcolony formation: A novel biofilm model of *Pseudomonas aeruginosa* for the cystic fibrosis lung. *Journal of Medical Microbiology*, *54*(7), 667–676. https://doi.org/10.1099/jmm.0.45969-0

Stressmann, F. A., Rogers, G. B., Marsh, P., Lilley, A. K., Daniels, T. W. V., Carroll, M. P., Hoffman, L. R., Jones, G., Allen, C. E., Patel, N., Forbes, B., Tuck, A., & Bruce, K. D. (2011). Does bacterial density in cystic fibrosis sputum increase prior to pulmonary exacerbation? *Journal of Cystic Fibrosis*, *10*(5), 357–365. https://doi.org/10.1016/j.jcf.2011.05.002

Stuart Elborn, J., Geller, D. E., Conrad, D., Aaron, S. D., Smyth, A. R., Fischer, R., Kerem, E., Bell, S. C., Loutit, J. S., Dudley, M. N., Morgan, E. E., VanDevanter, D. R., & Flume, P. A. (2015). A phase 3, open-label, randomized trial to evaluate the safety and efficacy of levofloxacin inhalation solution (APT-1026) versus tobramycin inhalation solution in stable cystic fibrosis patients. *Journal of Cystic Fibrosis*, *14*(4), 507–514. https://doi.org/10.1016/j.jcf.2014.12.013

Tavernier, S., Crabbé, A., Hacioglu, M., Stuer, L., Henry, S., Rigole, P., Dhondt, I., & Coenye, T. (2017). Community Composition Determines Activity of Antibiotics against Multispecies Biofilms. *Antimicrobial Agents and Chemotherapy*, *61*(9), e00302-17. https://doi.org/10.1128/AAC.00302-17

Theilmann, R. J., Darquenne, C., Elliott, A. R., Bailey, B. A., & Conrad, D. J. (2016). Characterizing Lung Disease in Cystic Fibrosis with Magnetic Resonance Imaging and Airway Physiology. *PLOS ONE*, *11*(6), e0157177. https://doi.org/10.1371/journal.pone.0157177

Thornton, C. S., Carmody, L. A., Kalikin, L. M., Opron, K., Caverly, L. J., & LiPuma, J. J. (2023). Airway bacterial community composition in persons with advanced cystic fibrosis lung disease. *Journal of Cystic Fibrosis*, *22*(4), 623–629. https://doi.org/10.1016/j.jcf.2023.01.001

Twomey, K. B., Alston, M., An, S.-Q., O'Connell, O. J., McCarthy, Y., Swarbreck, D., Febrer, M., Dow, J. M., Plant, B. J., & Ryan, R. P. (2013). Microbiota and metabolite profiling reveal specific alterations in bacterial community structure and environment in the cystic fibrosis airway during exacerbation. *PloS One*, *8*(12), e82432. https://doi.org/10.1371/journal.pone.0082432

Venkataranganayaka Abhilasha, K., & Kedihithlu Marathe, G. (2021). Bacterial lipoproteins in sepsis. *Immunobiology*, *226*(5), 152128. https://doi.org/10.1016/j.imbio.2021.152128

Vicary, A., Newkirk, H., Moreland, R., Gonzalez, C. F., Liu, M., Ramsey, J., & Leavitt, J. (2020). Complete Genome Sequence of *Stenotrophomonas maltophilia* Myophage Moby. *Microbiology Resource Announcements*, *9*(1), e01422-19. https://doi.org/10.1128/MRA.01422-19

Virtanen, P., Gommers, R., Oliphant, T. E., Haberland, M., Reddy, T., Cournapeau, D., Burovski, E., Peterson, P., Weckesser, W., Bright, J., van der Walt, S. J., Brett, M., Wilson, J., Millman, K. J., Mayorov, N., Nelson, A. R. J., Jones, E., Kern, R., Larson, E., … SciPy 1.0 Contributors. (2020). SciPy 1.0: Fundamental algorithms for scientific computing in Python. *Nature Methods*, *17*(3), 261–272. https://doi.org/10.1038/s41592-019-0686-2

Waskom, M. L. (2021). seaborn: Statistical data visualization. *Journal of Open Source Software*, *6*(60), 3021. https://doi.org/10.21105/joss.03021

Whiteson, K. L., Bailey, B., Bergkessel, M., Conrad, D., Delhaes, L., Felts, B., Harris, J. K., Hunter, R., Lim, Y. W., Maughan, H., Quinn, R., Salamon, P., Sullivan, J., Wagner, B. D., & Rainey, P. B. (2014). The Upper Respiratory Tract as a Microbial Source for Pulmonary Infections in Cystic Fibrosis. Parallels from Island Biogeography. *American Journal of Respiratory and Critical Care Medicine*, *189*(11), 1309–1315. https://doi.org/10.1164/rccm.201312-2129PP

Whiteson, K. L., Meinardi, S., Lim, Y. W., Schmieder, R., Maughan, H., Quinn, R., Blake, D. R., Conrad, D., & Rohwer, F. (2014a). Breath gas metabolites and bacterial metagenomes from cystic fibrosis airways indicate active pH neutral 2,3-butanedione fermentation. *The ISME Journal*, *8*(6), 1247–1258. https://doi.org/10.1038/ismej.2013.229

Whiteson, K. L., Meinardi, S., Lim, Y. W., Schmieder, R., Maughan, H., Quinn, R., Blake, D. R., Conrad, D., & Rohwer, F. (2014b). Breath gas metabolites and bacterial metagenomes from cystic fibrosis airways indicate active pH neutral 2,3-butanedione fermentation. *The ISME Journal*, *8*(6), 1247–1258. https://doi.org/10.1038/ismej.2013.229

Williams, S. R., Gebhart, D., Martin, D. W., & Scholl, D. (2008). Retargeting R-type pyocins to generate novel bactericidal protein complexes. *Applied and Environmental Microbiology*, *74*(12), 3868–3876. https://doi.org/10.1128/AEM.00141-08

Willner, D., Furlan, M., Haynes, M., Schmieder, R., Angly, F. E., Silva, J., Tammadoni, S., Nosrat, B., Conrad, D., & Rohwer, F. (2009). Metagenomic Analysis of

Respiratory Tract DNA Viral Communities in Cystic Fibrosis and Non-Cystic Fibrosis Individuals. *PLoS ONE*, *4*(10), e7370. https://doi.org/10.1371/journal.pone.0007370

Willner, D., Haynes, M. R., Furlan, M., Hanson, N., Kirby, B., Lim, Y. W., Rainey, P. B., Schmieder, R., Youle, M., Conrad, D., & Rohwer, F. (2012). Case Studies of the Spatial Heterogeneity of DNA Viruses in the Cystic Fibrosis Lung. *American Journal of Respiratory Cell and Molecular Biology*, *46*(2), 127–131. https://doi.org/10.1165/rcmb.2011-0253OC

Willner, D., Haynes, M. R., Furlan, M., Schmieder, R., Lim, Y. W., Rainey, P. B., Rohwer, F., & Conrad, D. (2012). Spatial distribution of microbial communities in the cystic fibrosis lung. *The ISME Journal*, *6*(2), 471–474. https://doi.org/10.1038/ismej.2011.104

Winzig, F., Gandhi, S., Lee, A., Würstle, S., Stanley, G. L., Capuano, I., Neuringer, I., Koff, J. L., Turner, P. E., & Chan, B. K. (2022). Inhaled Bacteriophage Therapy for Multi-Drug Resistant *Achromobacter*. *The Yale Journal of Biology and Medicine*, *95*(4), 413–427.

Wood, D. E., Lu, J., & Langmead, B. (2019). Improved metagenomic analysis with Kraken 2. *Genome Biology*, *20*(1), 257. https://doi.org/10.1186/s13059-019-1891-0

Worlitzsch, D., Tarran, R., Ulrich, M., Schwab, U., Cekici, A., Meyer, K. C., Birrer, P., Bellon, G., Berger, J., Weiss, T., Botzenhart, K., Yankaskas, J. R., Randell, S., Boucher, R. C., & Döring, G. (2002). Effects of reduced mucus oxygen concentration in airway *Pseudomonas* infections of cystic fibrosis patients. *Journal of Clinical Investigation*, *109*(3), 317–325. https://doi.org/10.1172/JCI0213870

Yamada, T., & Carlsson, J. (1975). Regulation of lactate dehydrogenase and change of fermentation products in streptococci. *Journal of Bacteriology*, *124*(1), 55–61. https://doi.org/10.1128/jb.124.1.55-61.1975

Zarei, S., Mirtar, A., Rohwer, F., Conrad, D. J., Theilmann, R. J., & Salamon, P. (2012). Mucus Distribution Model in a Lung with Cystic Fibrosis. *Computational and Mathematical Methods in Medicine*, *2012*, 1–8. https://doi.org/10.1155/2012/970809

Zarei, S., Mirtar, A., Rohwer, F., & Salamon, P. (2014). Stochastic Tracking of Infection in a CF Lung. *PLoS ONE*, *9*(10), e111245. https://doi.org/10.1371/journal.pone.0111245